As originally published in the IPC APEX EXPO Conference Proceedings.

NASA-DoD Lead-Free Electronics Project: Mechanical Shock Test

Thomas A. Woodrow, Ph.D.
Boeing Research and Technology
Seattle, WA

Abstract
Mechanical shock testing was conducted by Boeing Research and Technology (Seattle) for the NASA-DoD Lead-Free Electronics Solder Project. This project is follow-on to the Joint Council on Aging Aircraft/Joint Group on Pollution Prevention (JCAA/JG-PP) Lead-Free Solder Project which was the first group to test the reliability of lead-free solder joints against the requirements of the aerospace/military community.

Twenty one test vehicles were subjected to the shock test conditions (in four batches). The Shock Response Spectrum (SRS) input was increased during the test after every 100 shock pulses in an effort to fail as many components as possible within the time allotted for the test.

The solder joints on the components were electrically monitored using event detectors and any solder joint failures were recorded on a Lab view-based data collection system. The number of shocks required to fail a given component attached with SnPb solder was then compared to the number of shocks required to fail the same component attached with lead-free solder.

A complete modal analysis was conducted on one test vehicle using a laser vibrometer system which measured velocities, accelerations, and displacements at one hundred points. The laser vibrometer data was used to determine the frequencies of the major modes of the test vehicle and the shapes of the modes. In addition, laser vibrometer data collected during the mechanical shock test was used to calculate the strains generated (using custom software).

After completion of the testing, all of the test vehicles were visually inspected and cross sections were made. Broken component leads and other unwanted failure modes were documented.

Introduction
The NASA-DoD Lead-Free Electronics Project was started in 2006 to determine whether lead-free solders and finishes (before and after rework) are suitable for use in high reliability electronics. The Project is managed by NASA. The NASA-DoD Lead-Free Electronics Project includes members from the U.S. Air Force, BAE Systems, Boeing, Celestica, Harris, Lockheed Martin, NASA, NAVSEA Warfare Centers (Crane), Raytheon, Rockwell-Collins, ACI, Lockheed Martin, and Texas Instruments, among others. This project is follow-on to the 2001 Joint Council on Aging Aircraft/Joint Group on Pollution Prevention (JCAA/JG-PP) Lead-Free Solder Project which was the first group to test the reliability of lead-free solder joints against the requirements of the aerospace/military community.

The Project members wrote a Project Plan (Reference 1) which describes the assembly of the test vehicles and the testing to be done. The testing includes thermal cycling, vibration, mechanical shock, combined vibration/thermal cycling, and copper dissolution testing.

The objective of this study was to determine the effects of mechanical shock environments on the relative reliability of lead-free and tin/lead solder joints (i.e., which solder survived the longest). Modal data and strain data were also collected during this study in an effort to provide data that would be useful to those that may want to try to model the behavior of the NASA-DoD test vehicle.

Approach
The test vehicle designed for this project was a six-layer circuit board 12.75 inches wide by 9 inches high by 0.090 inches thick (Figure 1). The design used 0.5 ounce copper and a laminate with a high glass transition temperature (Tg of 170 degrees C, Isola 370HR). The test vehicle was populated with 63 components consisting of ceramic leadless chip carriers (CLCC's), QFN's, Alloy 42 TSOP's, TQFP's, BGA's, CSP's, and PDIP's. The components contained internal wire bonds so that once mounted on the test vehicle, each component would complete an electrical circuit that could be monitored during testing. Failure of a solder joint would cause a break in the electrical circuit that could be detected by an event detector. Each test vehicle also had a daisy-chain of twelve 0.016 inch diameter plated thorough holes so that the reliability of the

holes could be determined. The plated through holes were filled with solder during the wave solder operation. Each component location on the test vehicles was given a unique reference designator number.

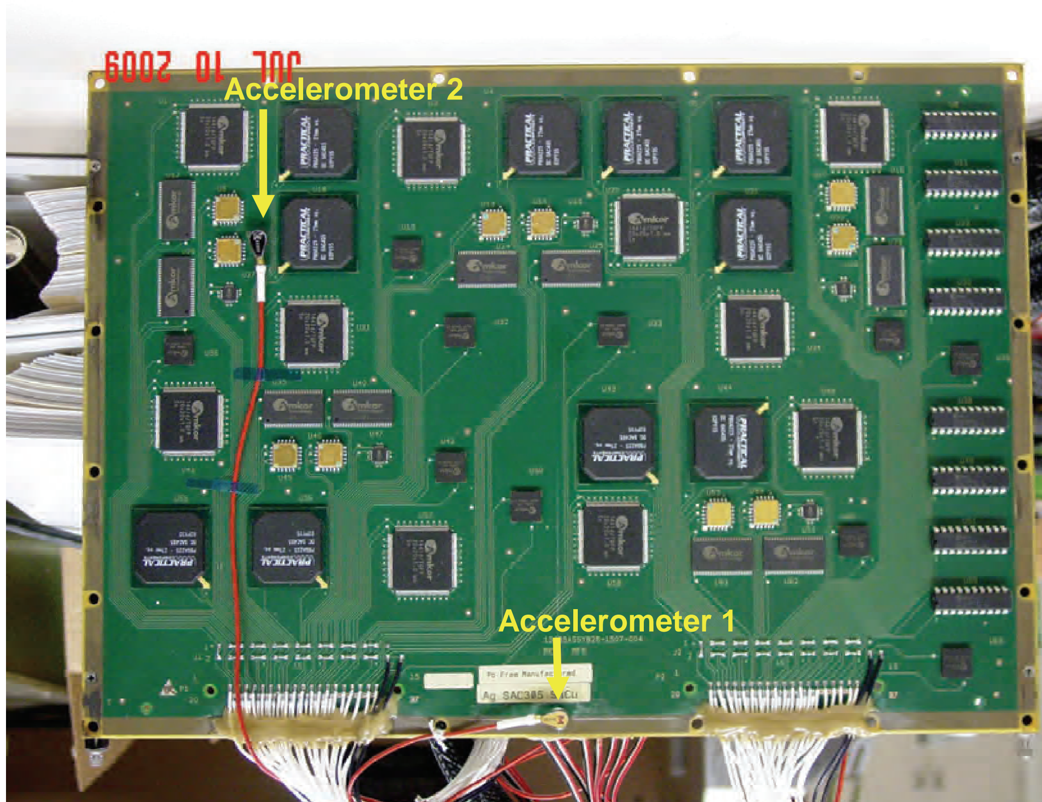

Figure 1. NASA-DoD Test Vehicle

The solder alloys selected for test were:

Sn3.0Ag0.5Cu paste for reflow soldering (abbreviated as SAC305)
Sn0.7Cu0.05Ni for wave soldering and as a paste for reflow soldering (abbreviated as SN100C)
Sn37Pb for reflow and wave soldering (abbreviated as SnPb)
Sn4.0Ag0.5Cu for BGA balls (abbreviated as SAC405)
Sn1.0Ag0.5Cu for CSP balls (abbreviated as SAC105)

The SAC305 alloy was chosen because it is currently the preferred alloy for use in lead-free commercial electronics. The SN100C alloy was chosen because it has been widely used in Asia with good results. SAC405 and SAC105 are alloys commonly used in the balls on area array devices. Finally, eutectic SnPb was included to act as the control alloy.

The test vehicles were divided into two types, i.e., "Manufactured" test vehicles and "Rework" test vehicles. Both types were made using an immersion silver board finish (although an ENIG PWB finish was used on a few test vehicles). The lead-free "Manufactured" and "Rework" test vehicles were assembled using lead-free solders and lead-free reflow and wave soldering profiles. The SnPb "Manufactured" and "Rework" test vehicles were assembled using eutectic SnPb solder and SnPb reflow and wave soldering profiles and were used as the controls. A 5-mil laser cut stencil was used during paste application.

As the name suggests, selected components on the "Rework" test vehicles were reworked. The components were removed; residual solder was cleaned from the pads using solder wick; and new components were attached using either SnPb or lead-free solder.

The "Rework" test vehicles were also populated with a number of mixed technology components (i.e., SnPb paste combined with a lead-free component finish or lead-free paste combined with a SnPb component finish).

The CLCC's with a lead-free pad finish were produced by dipping of gold-plated CLCC's into the respective molten solders. In addition, some tin-plated TQFP's were dipped into either molten SnPb or molten SAC305 to simulate a tin whisker mitigation process.

The component finishes used included SnPb, matte Sn, SnBi, SAC305, SAC405, and SAC105.

Table 1 lists the components used on the SnPb and lead-free "Manufactured" test vehicles; the finish on each component; and the solders used.

Table 2 lists the components used on the SnPb and lead-free "Rework" test vehicles; the finish on each component; the solders used; and which components were actually reworked.

Table 1. Assembly Matrix for "Manufactured" Mechanical Shock Test Vehicles

		SnPb "Manufactured" Test Vehicles			Pb-Free "Manufactured" Test Vehicles		
RefDes	Component	Component Finish	Reflow Solder Alloy	Wave Solder Alloy	Component Finish	Reflow Solder Alloy	Wave Solder Alloy
U18	BGA-225	SnPb	SnPb		SAC405	SAC305	
U43	BGA-225	SnPb	SnPb		SAC405	SAC305	
U04	BGA-225	SnPb	SnPb		SAC405	SAC305	
U06	BGA-225	SnPb	SnPb		SAC405	SAC305	
U55	BGA-225	SnPb	SnPb		SAC405	SAC305	
U02	BGA-225	SnPb	SnPb		SAC405	SAC305	
U05	BGA-225	SnPb	SnPb		SAC405	SAC305	
U21	BGA-225	SnPb	SnPb		SAC405	SAC305	
U44	BGA-225	SnPb	SnPb		SAC405	SAC305	
U56	BGA-225	SnPb	SnPb		SAC405	SAC305	
U09	CLCC-20	SnPb	SnPb		SAC305	SAC305	
U13	CLCC-20	SnPb	SnPb		SAC305	SAC305	
U22	CLCC-20	SnPb	SnPb		SAC305	SAC305	
U46	CLCC-20	SnPb	SnPb		SAC305	SAC305	
U53	CLCC-20	SnPb	SnPb		SAC305	SAC305	
U10	CLCC-20	SnPb	SnPb		SAC305	SAC305	
U14	CLCC-20	SnPb	SnPb		SAC305	SAC305	
U17	CLCC-20	SnPb	SnPb		SAC305	SAC305	
U45	CLCC-20	SnPb	SnPb		SAC305	SAC305	
U52	CLCC-20	SnPb	SnPb		SAC305	SAC305	
U32	CSP-100	SnPb	SnPb		SAC105	SAC305	
U33	CSP-100	SnPb	SnPb		SAC105	SAC305	
U35	CSP-100	SnPb	SnPb		SAC105	SAC305	
U50	CSP-100	SnPb	SnPb		SAC105	SAC305	
U63	CSP-100	SnPb	SnPb		SAC105	SAC305	
U19	CSP-100	SnPb	SnPb		SAC105	SAC305	
U36	CSP-100	SnPb	SnPb		SAC105	SAC305	
U37	CSP-100	SnPb	SnPb		SAC105	SAC305	
U42	CSP-100	SnPb	SnPb		SAC105	SAC305	
U60	CSP-100	SnPb	SnPb		SAC105	SAC305	
U08	PDIP-20	SnPb		SnPb	See Reference 2		SN100C
U23	PDIP-20	SnPb		SnPb	See Reference 2		SN100C
U49	PDIP-20	SnPb		SnPb	See Reference 2		SN100C
U59	PDIP-20	SnPb		SnPb	See Reference 2		SN100C
U30	PDIP-20	SnPb		SnPb	See Reference 2		SN100C
U38	PDIP-20	SnPb		SnPb	See Reference 2		SN100C
U11	PDIP-20	SnPb		SnPb	See Reference 2		SN100C
U51	PDIP-20	SnPb		SnPb	See Reference 2		SN100C
U15	QFN-20	SnPb	SnPb		Matte Sn	SAC305	
U27	QFN-20	SnPb	SnPb		Matte Sn	SAC305	
U28	QFN-20	SnPb	SnPb		Matte Sn	SAC305	
U47	QFN-20	SnPb	SnPb		Matte Sn	SAC305	
U54	QFN-20	SnPb	SnPb		Matte Sn	SAC305	
U01	TQFP-144	Matte Sn	SnPb		Matte Sn	SAC305	
U07	TQFP-144	Matte Sn	SnPb		Matte Sn	SAC305	
U20	TQFP-144	Matte Sn	SnPb		Matte Sn	SAC305	
U41	TQFP-144	Matte Sn	SnPb		Matte Sn	SAC305	
U58	TQFP-144	Matte Sn	SnPb		Matte Sn	SAC305	
U03	TQFP-144	Matte Sn	SnPb		Matte Sn	SAC305	
U31	TQFP-144	Matte Sn	SnPb		Matte Sn	SAC305	
U34	TQFP-144	Matte Sn	SnPb		Matte Sn	SAC305	
U48	TQFP-144	Matte Sn	SnPb		Matte Sn	SAC305	
U57	TQFP-144	Matte Sn	SnPb		Matte Sn	SAC305	
U12	TSOP-50	SnPb	SnPb		Sn	SAC305	
U25	TSOP-50	SnPb	SnPb		Sn	SAC305	
U29	TSOP-50	SnPb	SnPb		Sn	SAC305	
U39	TSOP-50	SnPb	SnPb		Sn	SAC305	
U61	TSOP-50	SnPb	SnPb		Sn	SAC305	
U16	TSOP-50	SnPb	SnPb		SnBi	SAC305	
U24	TSOP-50	SnPb	SnPb		SnBi	SAC305	
U26	TSOP-50	SnPb	SnPb		SnBi	SAC305	
U40	TSOP-50	SnPb	SnPb		SnBi	SAC305	
U62	TSOP-50	SnPb	SnPb		SnBi	SAC305	

Table 2. Assembly Matrix for "Rework" Mechanical Shock Test Vehicles

		SnPb "Rework" Test Vehicles					Pb-Free "Rework" Test Vehicles				
RefDes	Component	Original Component Finish	Reflow Solder Alloy	Wave Solder Alloy	New Component Finish	Rework Solder	Component Finish	Reflow Solder Alloy	Wave Solder Alloy	New Component Finish	Rework Solder
U04	BGA-225	SAC405	SnPb				SnPb	SAC305			
U55	BGA-225	SAC405	SnPb				SnPb	SAC305			
U05	BGA-225	SAC405	SnPb				SnPb	SAC305			
U44	BGA-225	SAC405	SnPb				SnPb	SAC305			
U18	BGA-225	SnPb	SnPb		SAC405	SnPb	SAC405	SAC305		SAC405	SnPb
U43	BGA-225	SnPb	SnPb		SAC405	SnPb	SAC405	SAC305		SAC405	SnPb
U06	BGA-225	SnPb	SnPb		SAC405	SnPb	SAC405	SAC305		SAC405	SnPb
U02	BGA-225	SnPb	SnPb		SnPb	Flux Only	SAC405	SAC305		SAC405	Flux Only
U21	BGA-225	SnPb	SnPb		SnPb	Flux Only	SAC405	SAC305		SAC405	Flux Only
U56	BGA-225	SnPb	SnPb		SnPb	Flux Only	SAC405	SAC305		SAC405	Flux Only
U09	CLCC-20	SAC305	SnPb				SnPb	SAC305			
U10	CLCC-20	SAC305	SnPb				SnPb	SAC305			
U13	CLCC-20	SAC305	SnPb				SnPb	SAC305			
U14	CLCC-20	SAC305	SnPb				SnPb	SAC305			
U17	CLCC-20	SAC305	SnPb				SnPb	SAC305			
U22	CLCC-20	SAC305	SnPb				SnPb	SAC305			
U45	CLCC-20	SAC305	SnPb				SnPb	SAC305			
U46	CLCC-20	SAC305	SnPb				SnPb	SAC305			
U52	CLCC-20	SAC305	SnPb				SnPb	SAC305			
U53	CLCC-20	SAC305	SnPb				SnPb	SAC305			
U32	CSP-100	SAC105	SnPb				SnPb	SAC305			
U35	CSP-100	SAC105	SnPb				SnPb	SAC305			
U63	CSP-100	SAC105	SnPb				SnPb	SAC305			
U36	CSP-100	SAC105	SnPb				SAC105	SAC305			
U50	CSP-100	SnPb	SnPb		SnPb	Flux Only	SAC105	SAC305		SAC105	Flux Only
U19	CSP-100	SnPb	SnPb		SnPb	Flux Only	SAC105	SAC305		SAC105	Flux Only
U37	CSP-100	SnPb	SnPb		SnPb	Flux Only	SAC105	SAC305		SAC105	Flux Only
U33	CSP-100	SnPb	SnPb		SAC105	SnPb	SAC105	SAC305		SAC105	SnPb
U42	CSP-100	SnPb	SnPb		SAC105	SnPb	SAC105	SAC305		SAC105	SnPb
U60	CSP-100	SnPb	SnPb		SAC105	SnPb	SAC105	SAC305		SAC105	SnPb
U08	PDIP-20	NiPdAu		SnPb			Sn		SN100C		
U23	PDIP-20	NiPdAu		SnPb			Sn		SN100C		
U49	PDIP-20	NiPdAu		SnPb			Sn		SN100C		
U59	PDIP-20	Sn		SnPb			Sn		SN100C		
U30	PDIP-20	Sn		SnPb			Sn		SN100C		
U38	PDIP-20	Sn		SnPb			Sn		SN100C		
U11	PDIP-20	SnPb		SnPb	Sn	SnPb	Sn		SN100C	Sn	SN100C
U51	PDIP-20	SnPb		SnPb	Sn	SnPb	Sn		SN100C	Sn	SN100C
U15	QFN-20	Matte Sn	SnPb				SnPb	SAC305			
U27	QFN-20	Matte Sn	SnPb				SnPb	SAC305			
U28	QFN-20	Matte Sn	SnPb				SnPb	SAC305			
U47	QFN-20	Matte Sn	SnPb				SnPb	SAC305			
U54	QFN-20	Matte Sn	SnPb				SnPb	SAC305			
U03	TQFP-144	NiPdAu	SnPb				NiPdAu	SAC305			
U31	TQFP-144	NiPdAu	SnPb				NiPdAu	SAC305			
U34	TQFP-144	NiPdAu	SnPb				NiPdAu	SAC305			
U48	TQFP-144	NiPdAu	SnPb				NiPdAu	SAC305			
U57	TQFP-144	NiPdAu	SnPb				NiPdAu	SAC305			
U01	TQFP-144	SnPb Dip	SnPb				SAC 305 Dip	SAC305			
U07	TQFP-144	SnPb Dip	SnPb				SAC 305 Dip	SAC305			
U20	TQFP-144	SnPb Dip	SnPb				SAC 305 Dip	SAC305			
U41	TQFP-144	SnPb Dip	SnPb				SAC 305 Dip	SAC305			
U58	TQFP-144	SnPb Dip	SnPb				SAC 305 Dip	SAC305			
U29	TSOP-50	Sn	SnPb				SnBi	SAC305			
U39	TSOP-50	Sn	SnPb				SnBi	SAC305			
U61	TSOP-50	Sn	SnPb				SnBi	SAC305			
U16	TSOP-50	SnBi	SnPb				SnPb	SAC305			
U40	TSOP-50	SnBi	SnPb				SnPb	SAC305			
U62	TSOP-50	SnBi	SnPb				SnPb	SAC305			
U12	TSOP-50	SnPb	SnPb		SnPb	SnPb	Sn	SAC305		Sn	SnPb
U25	TSOP-50	SnPb	SnPb		SnPb	SnPb	Sn	SAC305		Sn	SnPb
U24	TSOP-50	SnPb	SnPb		Sn	SnPb	SnBi	SAC305		SnBi	SAC305
U26	TSOP-50	SnPb	SnPb		Sn	SnPb	SnBi	SAC305		SnBi	SAC305

Mixed SnPb/Pb-Free

Sn Plating Dipped for Whisker Mitigation

One hundred and ninety three test vehicles were assembled at BAE Systems in Irving, TX. One hundred and twenty of these test vehicles were "Manufactured" PWA's and seventy three were "Rework" PWA's. Eighteen components were reworked

on each of the “Rework” test vehicles (six BGA’s; six CSP’s; two PDIP’s; and four TSOP’s). In general, solder wire was used for reworking the components. The BGA’s and CSP’s, however, were replaced using flux only or by applying paste to the balls and then using a hot air rework station to form the solder joints (see Table 2). During rework of the BGA’s and CSP’s, a SnPb thermal profile was used for the SnPb “Rework” test vehicles and a Pb-free thermal profile was used on the Pb-free “Rework” test vehicles. The reflow profiles for initial assembly using either SnPb or the lead-free solder pastes are shown in Figures 2 and 3. Wave soldering with SnPb was done at BAE Systems and the lead-free wave soldering was done at Scorpio Solutions in Garfield Heights, Ohio. All rework was done at BAE Systems, Lockheed Martin, and Rockwell-Collins. Each rework site focused on the test vehicles for a specific test to eliminate effects due to site-to-site variations in rework procedures. The wave soldering and rework thermal profiles used can be found in Reference 2.

After assembly and rework, all test vehicles were thermally aged at 100°C for 24 hours. Twenty one test vehicles were then delivered to Boeing for mechanical shock testing. These consisted of 5 SnPb “Manufactured” test vehicles; 5 Pb-free “Manufactured” test vehicles; 6 SnPb “Rework” test vehicles; and 5 Pb-free “Rework” test vehicles. All of the test vehicles had an immersion silver PWB finish except for one SnPb “Rework” test vehicle (Test Vehicle 160) which had an ENIG PWB finish.

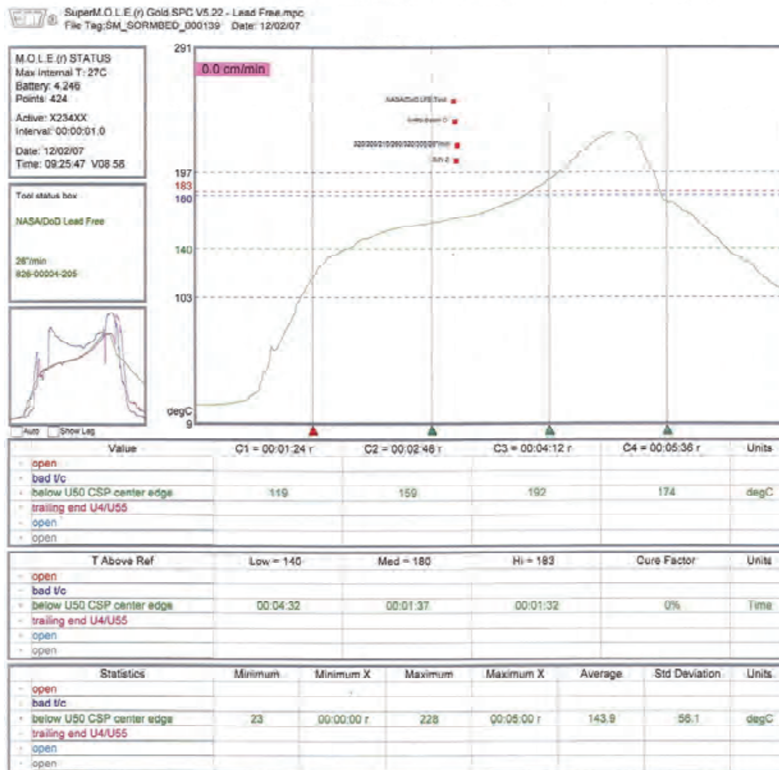

Source: BAE Systems

Figure 2. Reflow Profile for SnPb Solder Paste

On the SnPb “Rework” test vehicles, all of the CLCC’s were finished with SAC305 (on the pads and in the castellation) and assembled with SnPb paste which resulted in lead-free solder joints contaminated with Pb after assembly (see Table 2). In addition, some of the BGA’s combined SAC405 balls with SnPb solder paste which also resulted in lead-free solder joints contaminated with Pb (on reworked and unreworked BGA’s). Also, some of the CSP’s combined SAC105 balls with SnPb solder paste (reworked and unreworked). This mixing was done intentionally in order to determine the effects of lead-contamination upon lead-free solder reliability. Inductively coupled plasma (ICP) spectroscopy was used by Boeing to quantify the amount of Pb in these solder joints on one of the SnPb “Rework” test vehicles (see Table 3; Test Vehicle ID # 149). The solder joints were removed with a scalpel, dissolved in mixed nitric/hydrochloric acid, and the solution was analyzed by ICP spectroscopy.

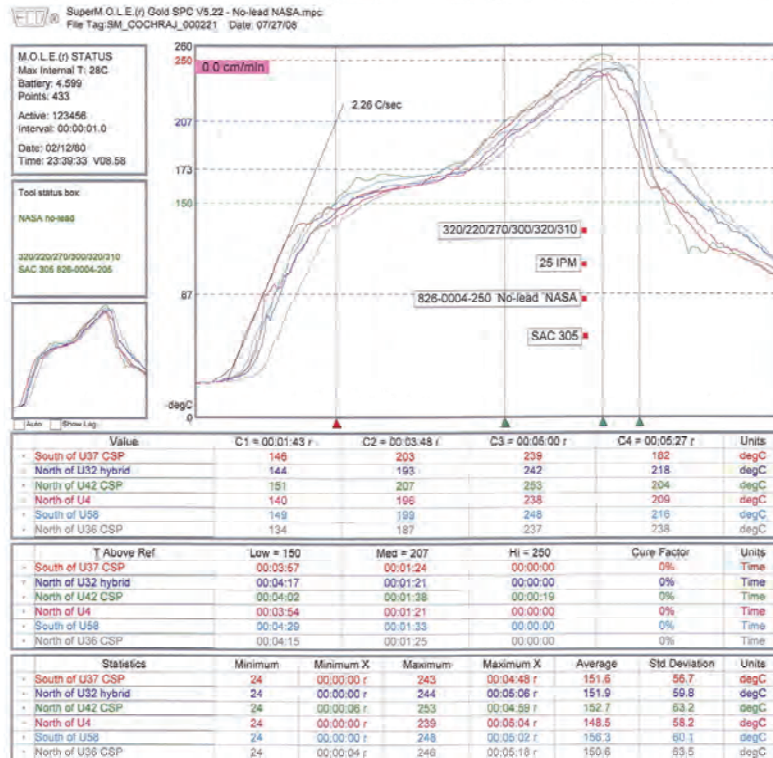

Source: BAE Systems

Figure 3. Reflow Profile for SAC305 Solder Paste

On the Pb-free "Rework" test vehicles, all of the CLCC's and QFN's were finished with SnPb and assembled with SAC305 paste which resulted in lead-free solder joints contaminated with Pb after assembly (see Table 2). In addition, some of the BGA's combined SnPb balls with SAC305 solder paste which also resulted in lead-free solder joints contaminated with Pb (on unreworked BGA's). Also, some of the CSP's combined SAC105 balls with SnPb solder paste (after rework). This mixing was done intentionally in order to determine the effects of lead-contamination upon lead-free solder reliability. Again, Inductively coupled plasma (ICP) spectroscopy was used by Boeing to quantify the amount of Pb in these solder joints on one of the Pb-Free "Rework" test vehicles (see Table 3; Test Vehicle ID # 193).

All of the ICP analyses appeared reasonable with the possible exception of the two TSOP's and the BGA U43 analyses. The copper content for these components were higher than expected. It is probable that copper was removed from the test vehicle pads along with the solder when the solder joints were cut from the test vehicle using a scapel.

Table 3. Chemical Analysis of Solder Joints Contaminated with Pb (by ICP Spectroscopy)

Component	Ref. Des.	Test Vehicle ID	Reworked?	Component Finish	Board Finish	Solder	%Ag	%Cu	%Pb	%Sn	%Bi	%Au
BGA-225	U04	149	No	SAC405	Ag	Sn37Pb	3.46	0.94	3.77	91.71	0.00	0.13
BGA-225	U04	193	No	Sn37Pb	Ag	SAC305	0.31	0.26	33.91	65.44	0.00	0.08
BGA-225	U43	193	Yes	SAC405	Residual SAC	Sn37Pb	3.13	3.18**	5.52	88.07	0.00	0.10
CLCC-20	U09	149	No	SAC305	Ag	Sn37Pb	1.35	0.49	24.68	73.48	0.00	0.00
CLCC-20	U09	193	No	Sn37Pb	Ag	SAC305	1.92	0.39	16.46	81.19	0.04	0.00
CSP-100*	U33	149	Yes	SAC105	Residual Sn37Pb	Sn37Pb	0.90	0.73	1.81	96.23	0.00	0.33
CSP-100*	U33	193	Yes	SAC105	Residual SAC	Sn37Pb	0.83	0.63	4.43	93.82	0.00	0.29
QFN-20	U15	193	No	SnPb	Ag	SAC305	3.39	0.85	0.93	94.83	0.00	0.00
TSOP-50	U16	149	No	SnBi	Ag	Sn37Pb	0.44	2.68**	35.73	61.06	0.09	0.00
TSOP-50	U16	193	No	SnPb	Ag	SAC305	3.53	6.10**	1.51	88.86	0.00	0.00

*PWB Cu pads had to be cut from the CSP balls. This operation also removed that end of each ball.
** Copper may have been removed from the PWB pads when the solder joints were cut from the test vehicle.

An aluminum fixture was built that could hold up to six test vehicles at one time. Slots were cut into the fixture to accept wedge locks (Calmark A260-8.80T2L) that were mounted on both ends of the test vehicles with screws. The wedge locks were designed with a special locking feature to prevent loosening from mechanical shock and were torqued to 8.5 in-lbs. Figure 4 shows the NASA-DoD test vehicles mounted in the test fixture.

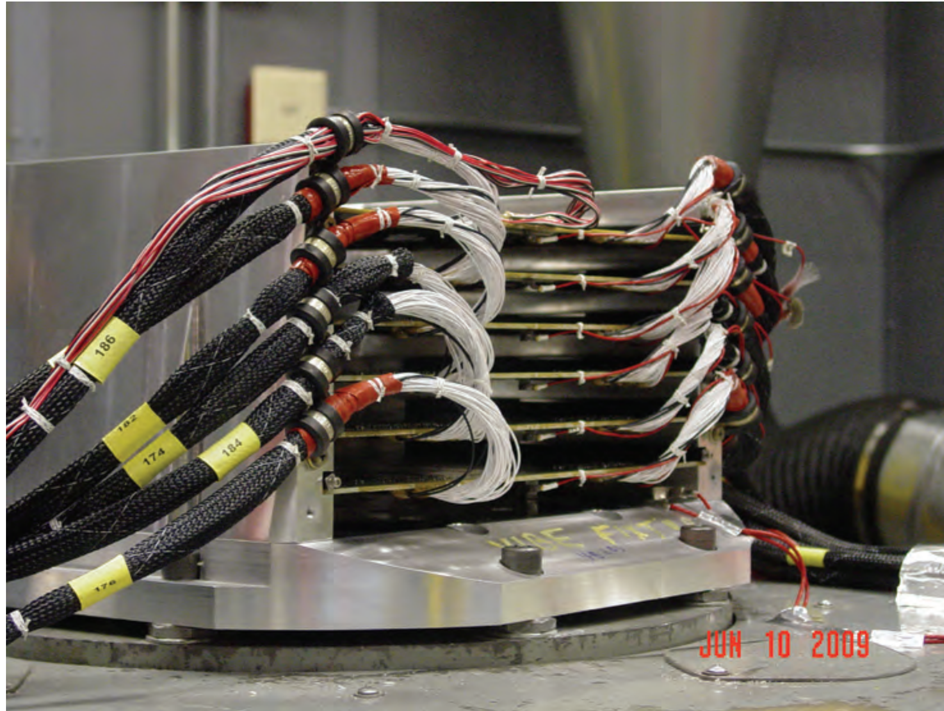

Figure 4. Test Vehicles in Fixture

The electrodynamics shaker used for the test was an Unholtz-Dickie T1000W with a 360 KW amplifier controlled by a Spectral Dynamics 2550B Vibration Controller. The shaker input was controlled by an accelerometer mounted near the bottom of the fixture.

Each “Manufactured” test vehicle was instrumented with two calibrated accelerometers as shown in Figure 1 for collecting acceleration data during the shock test. Accelerometer 1 was located at the point of maximum deflection for the first and second modes (70 and 94 Hz) and Accelerometer 2 was located at the point of maximum deflection for the seventh mode (391 Hz).

Four three-element stacked rosette strain gages were mounted on one test vehicle as shown in Figure 5 to collect strain data in the x and y directions at each test level.

A modal analysis was conducted on Test Vehicle 75 using a laser vibrometer system (Polytec Scanning Vibrometer, Waldbronn, Germany) which was suspended above the electrodynamics shaker. The laser vibrometer was used to measure velocities, accelerations, and displacements at 100 points on the bottom surface of a test vehicle during low level random vibration in the z-axis (the axis perpendicular to the plane of the test vehicle). The laser vibrometer measurements identified 4 major resonance frequencies for the NASA/DoD test vehicle at 70, 94, 391, and 998 Hz. The laser vibrometer data was also used to calculate a bending mode shape for each of the resonances (see Figure 6 for the mode shape of the first mode at 70 Hz). It was expected that the mechanical shock pulses would excite these bending modes which in turn would cause solder joint damage.

Laser vibrometer velocity data was also collected at 100 points on the surface of Test Vehicle 75 at several test levels during the mechanical shock test. This data was used to calculate full field peak strains in the vehicle x and y directions for all modes combined during a shock pulse (see the example in Figure 7). The calculations were performed using proprietary software developed by Millennium Dynamics Corporation (Acworth, GA). The regions of calculated maximum strain were down the centerline of the vehicle and along the edges of the vehicle (near the wedge locks). The calculated maximum strains compared well with the strain data from the strain gages. Note that the maximum strains generated across the test vehicle appear to be mostly caused by the first mode.

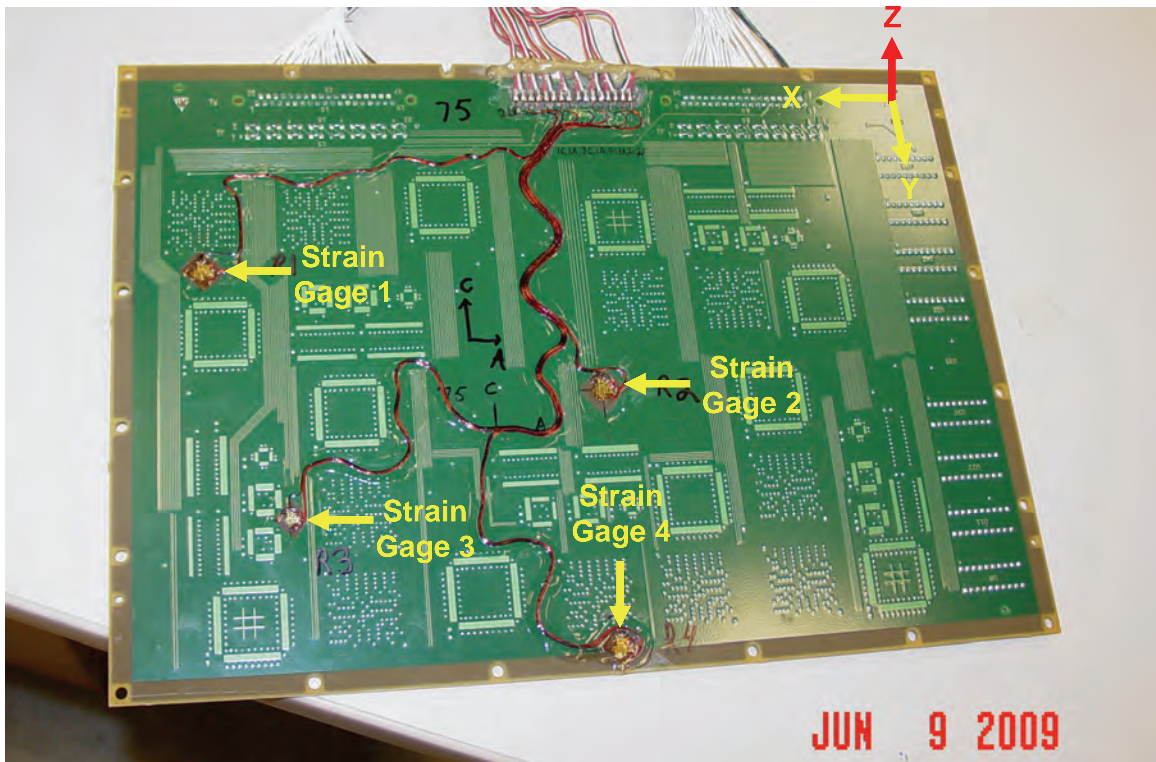

Figure 5. Strain Gage Placement on Test Vehicle 75

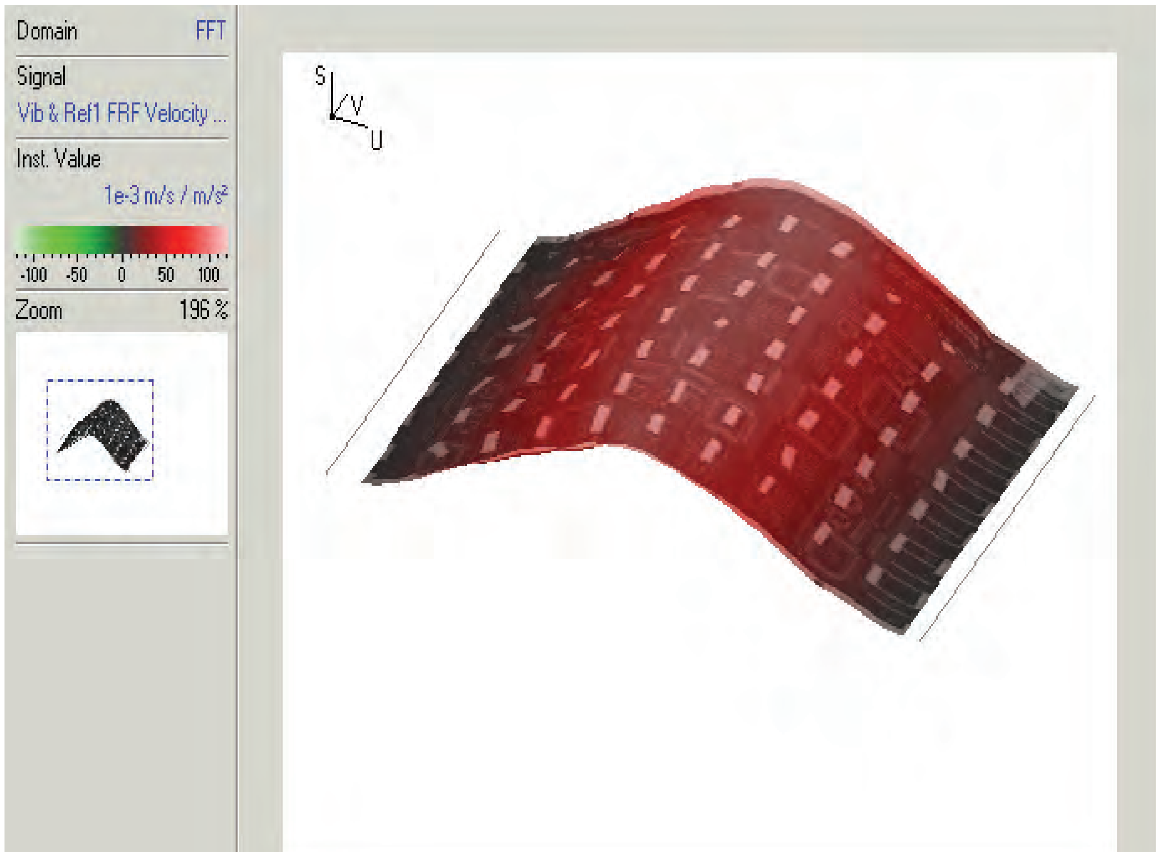

Figure 6. Mode Shape at 70 Hz

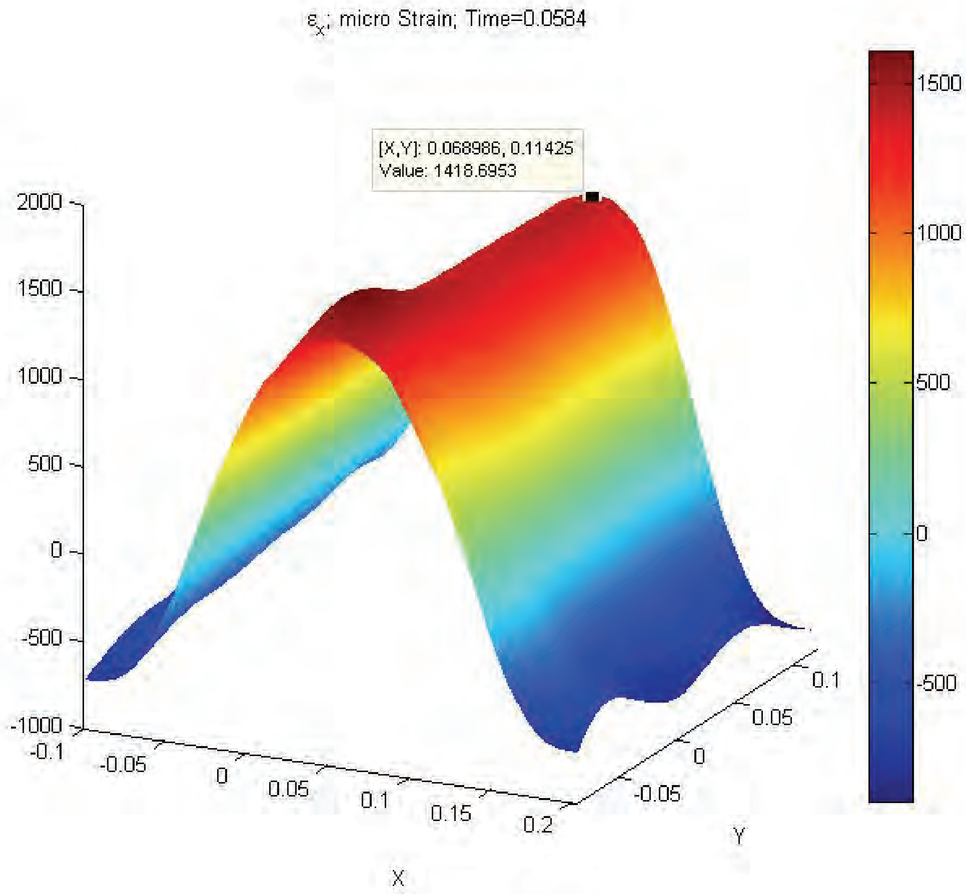

Figure 7. Peak Strains during 100 G Shock Pulse from All Modes Combined (x-direction, in micro strain)

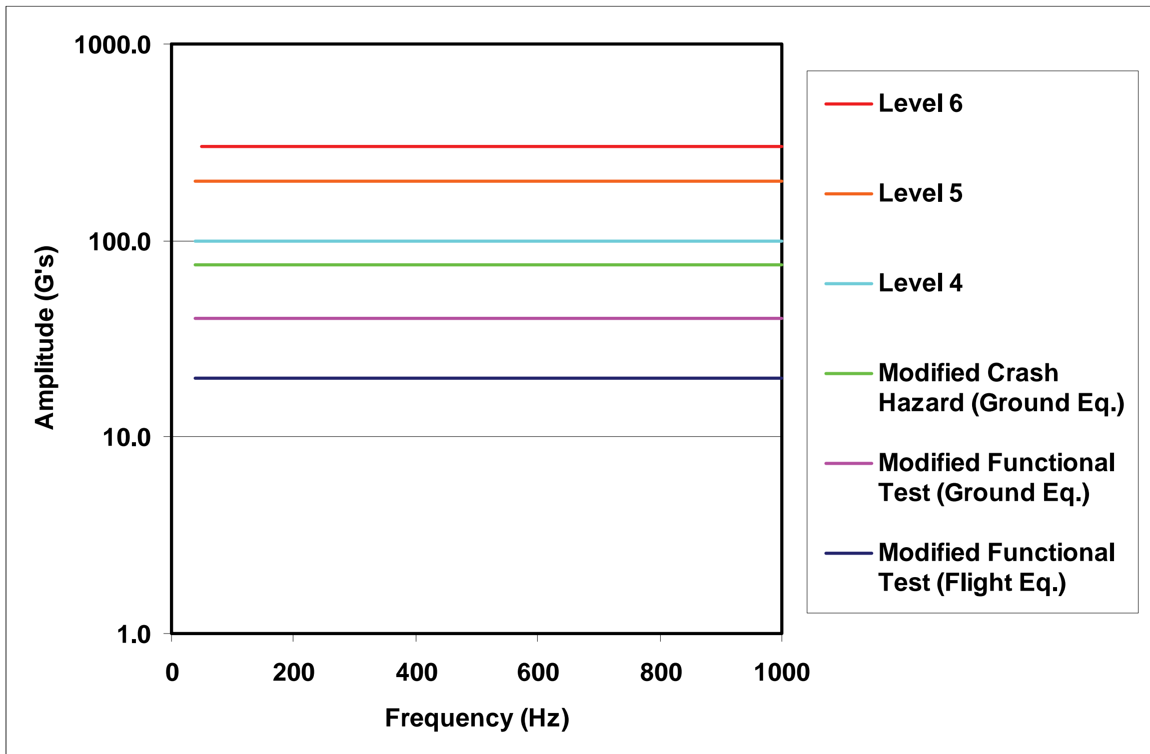

Figure 8. Mechanical Shock SRS Test Levels (5% Damping)

As originally published in the IPC APEX EXPO Conference Proceedings.

This demonstrates that the strain environment at a given location on a test vehicle can be very different from the strain environment at a different location on the same vehicle during the same test. This implies that the best practice is to directly compare identical components in identical locations on identical test vehicles. It also implies that the test solder must be used on one set of test vehicles and the control solder on a second set of test vehicles.

After collection of the modal and strain data, the test vehicles were subjected to a mechanical shock step stress test in the z-axis only (the direction perpendicular to the plane of the PWA). The 21 test vehicles were divided into four groups for testing, with each group containing both SnPb and Pb-free test vehicles.

At the first stress level, the test vehicles were subjected to 100 shock pulses using the 20 G Shock Response Spectrum (SRS) shown in Figure 8 (5% damping). The SRS was flat from 40 to 1000 Hz. This is a standard test (i.e., the Functional Test for Flight Equipment as defined in MIL-STD-810G Method 516.6) during which the test article is exposed to a minimum of three shock pulses. The 20 G SRS used was modified slightly from that shown in MIL-STD-810G (Reference 3). The modifications included lowering the cross-over frequency to 40 Hz to insure that the first resonance of the test vehicle was fully excited and reducing the terminal frequency to 1000 Hz.

At the second stress level, the test vehicles were subjected to 100 shock pulses using the 40 G Shock Response Spectrum (SRS) shown in Figure 8. This is a standard test (i.e., the Functional Test for Ground Equipment as defined in MIL-STD-810G Method 516.6) during which the test article is exposed to a minimum of three shock pulses.

At the third stress level, the test vehicles were subjected to 100 shock pulses using the 75 G Shock Response Spectrum (SRS) shown in Figure 8. This is a standard test (i.e., the Crash Hazard Test for Ground Equipment as defined in MIL-STD-810G Method 516.6) during which the test article is exposed to a minimum of three shock pulses.

The test vehicles were then exposed to 100 shock pulses using a 100 G SRS followed by 100 shock pulses using a 200 G SRS as shown in Figure 8 (Test Levels 4 and 5).

The mechanical shock test was concluded by exposing the test vehicles to 400 shock pulses using the 300 G SRS shown in Figure 8.

At the 300 G test level, the sides of the wedge locks began to gradually deform. Great care had to be taken to periodically tighten the wedge locks and to replace the wedge locks when the deformations reduced the clamping force of the wedge locks.

The 63 components and the PTH net on each test vehicle were individually monitored using Analysis Tech 256STD Event Detectors (set to a 300 ohm threshold) combined with Lab view-based data collection software. The wires connecting the test vehicle to the event detector had to be glued to the surface of the test vehicle (Figure 1) to prevent them from flexing and breaking during the mechanical shock test. In addition, the wire bundles from the test vehicle were firmly clamped to the fixture in order to prevent flexing and breaking of the wires. All wire bundles were covered with a grounded metallic shield to prevent electrical noise from the shaker from interfering with the event detectors.

The accelerometer data recorded at each test level included: the SRS inputs into the fixture; the pulse shape and amplitudes used for each test level; and the response of each "Manufactured" test vehicle. Representative accelerometer data for the 20 G test level is shown in Figures 9 through 11. At each test level, the same pulse shape was used for each of the shock pulses. The use of an electrodynamics shaker insured that reproducible pulse shapes could be produced for each test level during testing of the four batches of test vehicles. It should be noted that the accelerations experienced by each test vehicle were much higher than the SRS accelerations input into the fixture. For example, during a 20 G shock pulse, the centerline of Test Vehicle 30 was actually accelerating at 168 G (at 70 Hz) (see Figure 11).

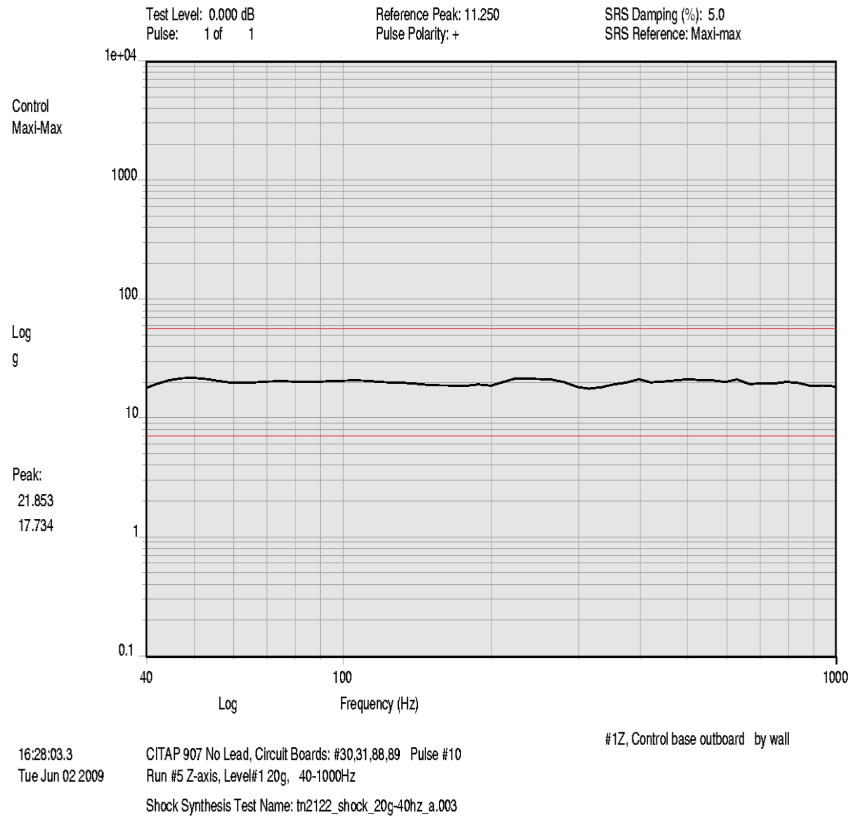

Figure 9. 20 G SRS Input (Accelerometer on Fixture)

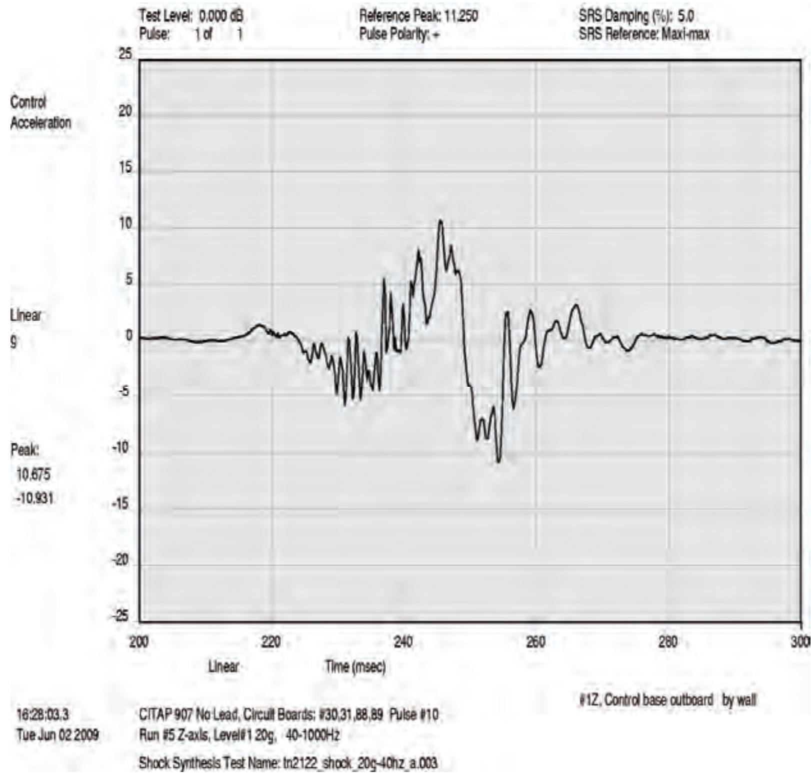

Figure 10. Pulse Used to Create 20 G SRS Input (Accelerometer on Fixture)

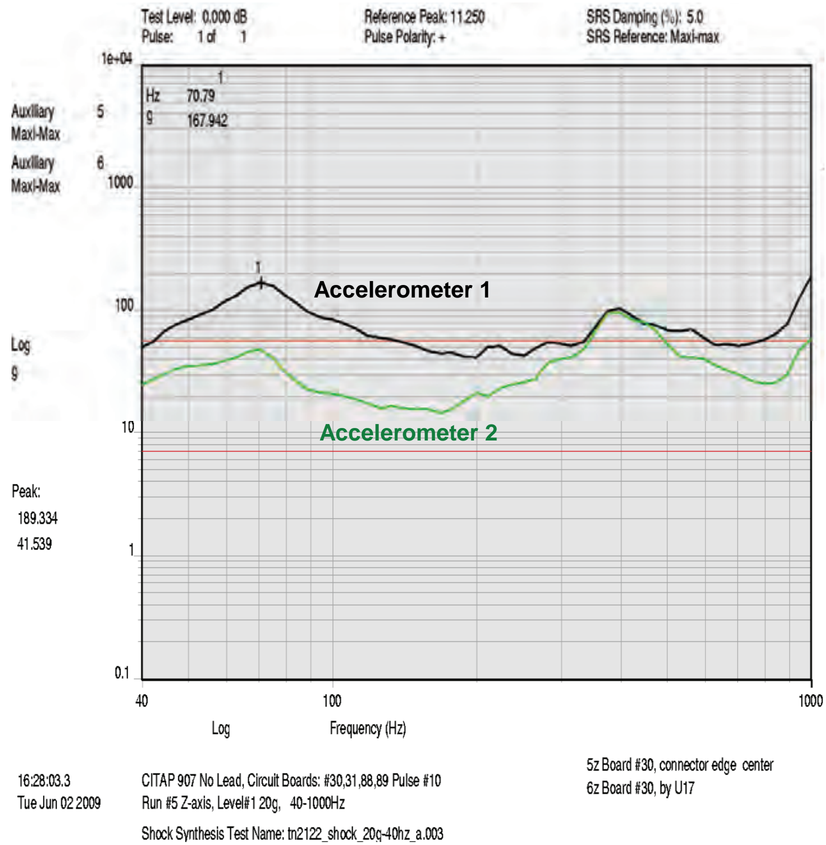

Figure 11. Test Vehicle SRS Response to 20 G SRS Input (Test Vehicle 30)

Figure 12 shows the time history response of Strain Gage 2 after a 20 G shock pulse. The initial shock pulse deflects the test vehicle in one direction and the test vehicle then oscillates back and forth until the acceleration imparted by the pulse decays to zero. Table 4 shows the peak strain readings from the four strain gages on Test Vehicle 75 at every test level (in the x and y board directions).

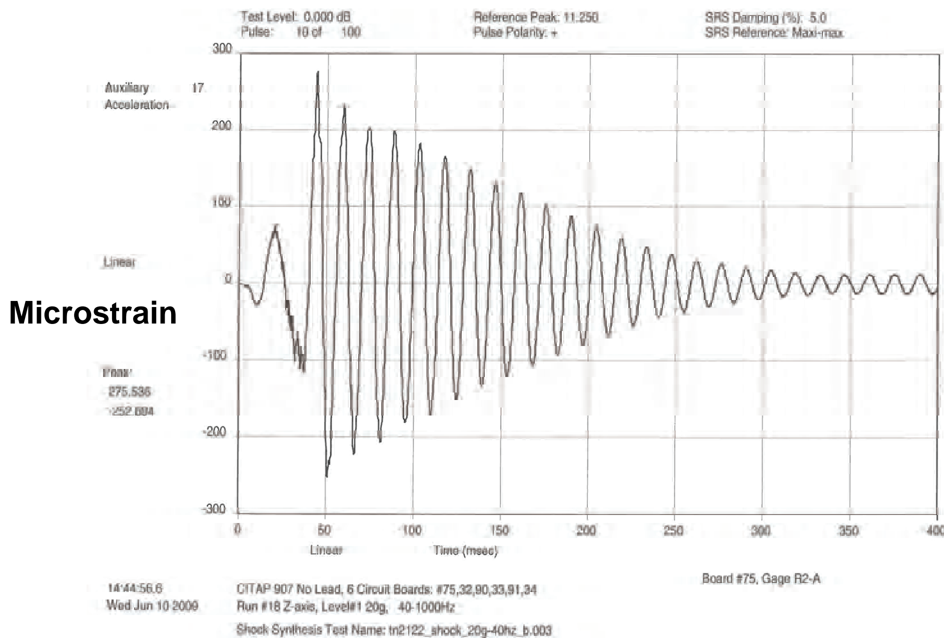

Figure 12. Test Vehicle Time History Strain Response to 20 G SRS Input (Strain Gage 2, x-Direction)

Table 4. Maximum Strain Gage Readings for All SRS Test Levels (in micro strain)

SRS Test Level (G's)	Strain Gage 1 x-Direction	Strain Gage 1 y-Direction	Strain Gage 2 x-Direction	Strain Gage 2 y-Direction	Strain Gage 3 x-Direction	Strain Gage 3 y-Direction	Strain Gage 4 x-Direction	Strain Gage 4 y-Direction
20	-153	-64	276	-47	-77	-14	265	-3
40	462	-180	760	-108	183	-63	754	-11
75	568	-282	1274	-168	355	111	1180	-18
100	655	-304	1434	-171	408	-126	1350	-27
200	715	-424	2376	-207	709	43	2209	-41
300	572	-597	2925	-224	1315	175	2967	-46

Results and Discussion

Table 5 shows the percent of each component type that failed on both the "Manufactured" and the "Rework" test vehicles at the end of the test. Notice that the QFN-20's and the TSOP-50's were resistant to failure due to mechanical shock.

Table 5. % of Components Failed (Includes Mixed Solders)

	% of Components Failed During Mechanical Shock Testing			
	"Manufactured" Test Vehicles		"Rework" Test Vehicles	
	SnPb	Pb-Free	SnPb	Pb-Free
Component				
BGA-225	94	96	95	100
CLCC-20	22	30	22	30
CSP-100	32	26	42	38
PDIP-20	53	73	54	58
QFN-20	0	10	0	0
TQFP-144	70	62	68	80
TSOP-50	4	0	22	20

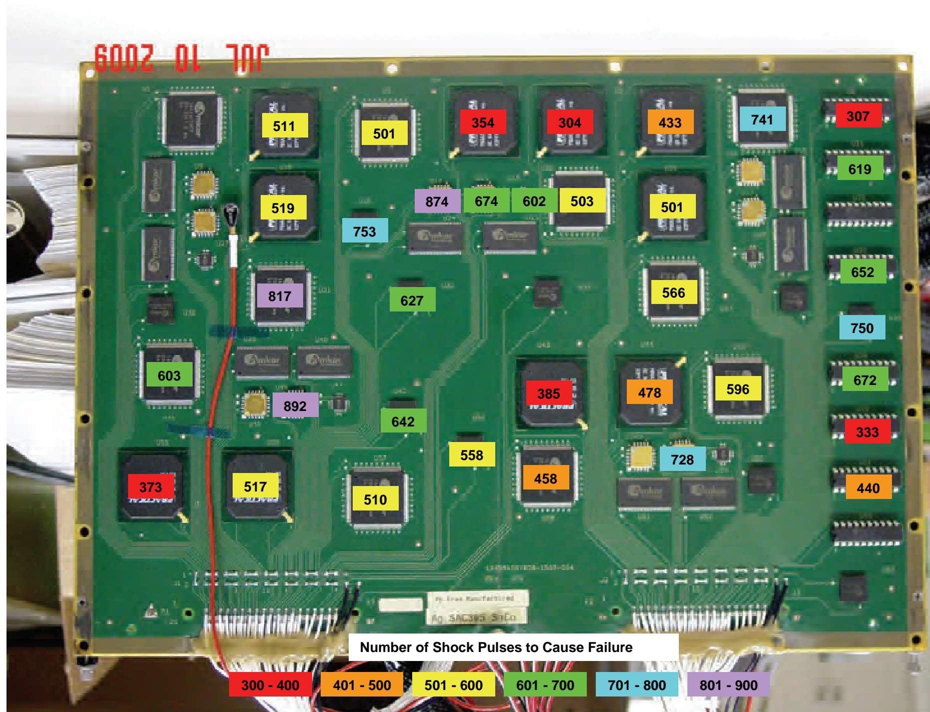

Figure 13. Number of Shocks Required to Fail Components on Test Vehicle 75

Figure 13 shows how many shock pulses were required to fail the components on a test vehicle. The failures are color coded according to how many shock pulses were required to cause the failure (red = 300 to 400 pulses; orange = 401 to 500 pulses;

yellow = 501 to 600 pulses; green = 601 to 700 pulses; blue = 701 to 800 pulses; and purple = 801 to 900 pulses). In general, the components tended to fail first down the centerline and along the edges of the test vehicle (near the wedgelocks). Therefore, the first component failures coincide with the regions of highest strain as shown in Figure 7.

After completion of all shock testing, the "Manufactured" and "Rework" test vehicles were visually inspected using a HYROX Hi-Scope Compact Micro Vision System (Model KH-2200 MD2). The main goal of the inspection was to document any broken or missing leads on leaded components. This was necessary so that failures due to solder joint cracking could be distinguished from failures due to lead breakage. The secondary goal of the inspection was to document any unusual solder joint failure modes. Some components (BCA's and CLCC's) tended to fall off of the test vehicles during testing. In addition, all wiring was visually inspected to verify that no signal wires had broken during the shock test (a broken signal wire would look like a solder joint failure to the event detectors). No broken signal wires were found. Microsections were also done to identify major failure modes.

It should be noted that all of the surface mount components survived 100 shock pulses at each of the first three test levels. This means that they effectively passed the Functional Test for Flight Equipment 33 times; they passed the Functional Test for Ground Equipment 33 times; and they passed the Crash Hazard Test for Ground Equipment 33 times. Therefore, the surface mount components soldered with SnPb and with SAC305 are both resistant to failure under mechanical shock.

At the more severe test levels, numerous components did fail electrically which allowed the relative reliability of the SnPb control solder and the lead-free solders to be compared.

The test results for each component type are presented in the following sections. The solder paste used is listed first followed by the component finish (for example, SAC305/SAC405 on a BGA is equivalent to SAC305 solder/SAC405 balls).

BGA-225's

The combination of SAC305 solder/SAC405 balls generally performed as well as the SnPb/SnPb controls in mechanical shock (see Figures 14, 15, and 16) although there were some early SAC305/SAC405 failures (see Figure 14). Microsections made at the end of the test showed that the corner solder joints failed first. The SnPb/SnPb microsections showed pad cratering, PWB trace cracking, and solder joint cracking on the component side. The SAC305/SAC405 microsections showed PWB trace cracking and solder joint cracking at the component side intermetallic layer. Which failure mechanism occurred first could not be determined from the microsections.

The combination of SAC305 solder/SnPb balls also performed as well as the SnPb/SnPb controls. In contrast, the combination of SnPb solder/SAC405 balls underperformed the controls (Figure 14) on either an immersion silver or ENIG board finish. These SnPb/SAC405 BGA's were reflowed using a SnPb reflow profile.

SnPb/SnPb BGA's reworked with flux only/SnPb balls and SAC305/SAC405 BGA's reworked with flux only/SAC 405 balls were as reliable as the SnPb/SnPb control BGA's (Figure 15).

SnPb/SnPb BGA's reworked with SnPb/SAC405 underperformed SAC305/SAC405 BGA's reworked with SnPb/SAC405 (Figure 16). The difference is probably because the former were reworked with a SnPb thermal profile while the latter were reworked with a Pb-free thermal profile which should have allowed complete mixing of the solders.

During rework of the lead-free BGA's, problems were encountered with electrical opens due to formation of poor solder joints. This required that some lead-free BGA's be reworked several times instead of just once. In general, multiple rework cycles did not appear to have a negative effect on the performance of the lead-free solder joints relative to their unreworked counterparts.

A number of BGA's fell off of the test vehicles during the shock test which allowed the failure mechanisms to be examined more closely.

Surprisingly, on the SnPb/SnPb BGA's that fell off, almost 100% of the solder joints failed by pad cratering. The BGA balls and associated PWB copper pads were missing from the test vehicles (Figure 17).

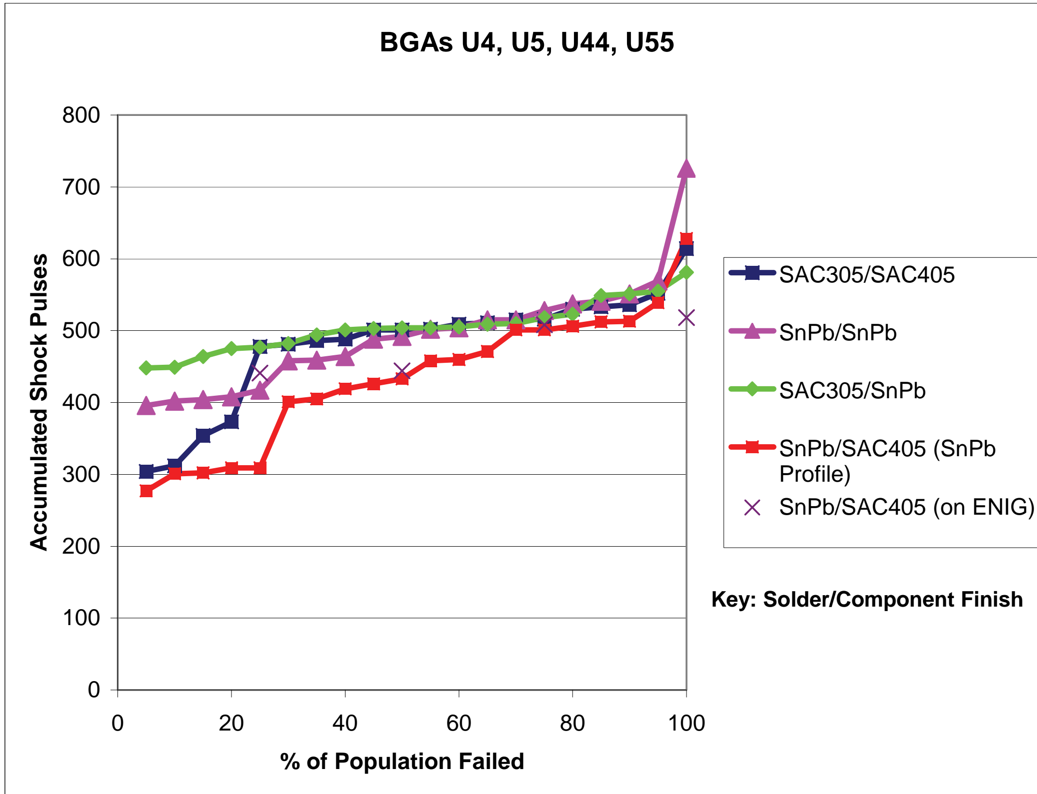

Figure 14. Combined Data from BGA's U4, U5, U44, and U55

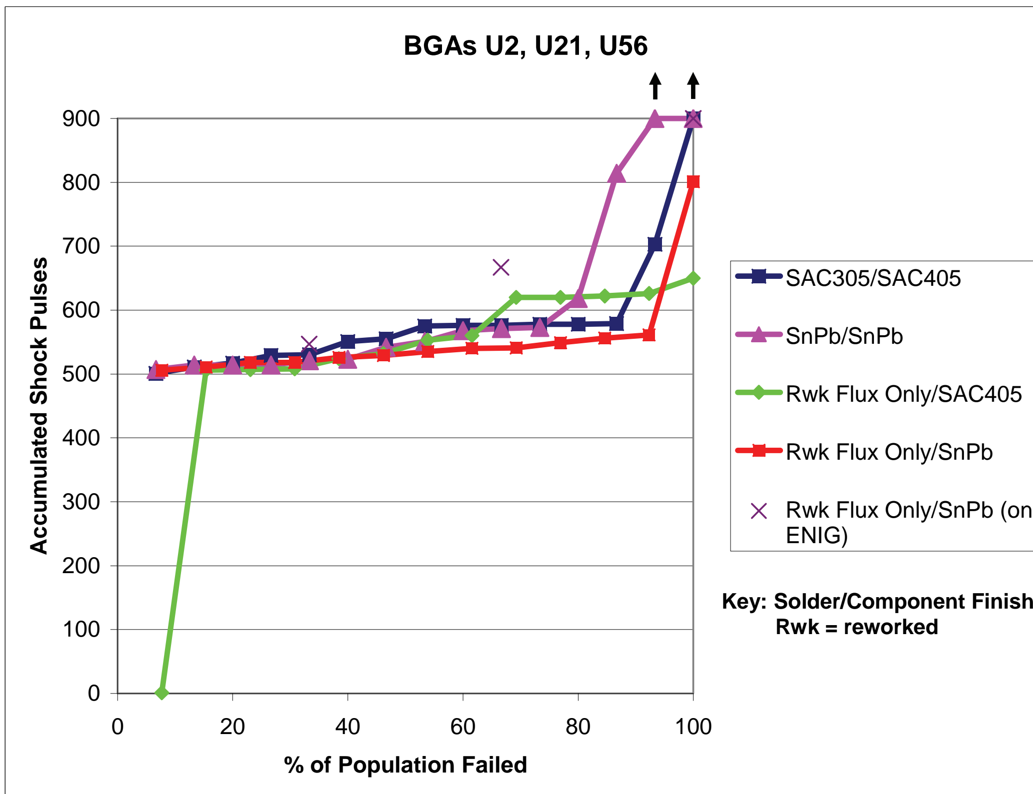

Figure 15. Combined Data from BGA's U2, U21, and U56

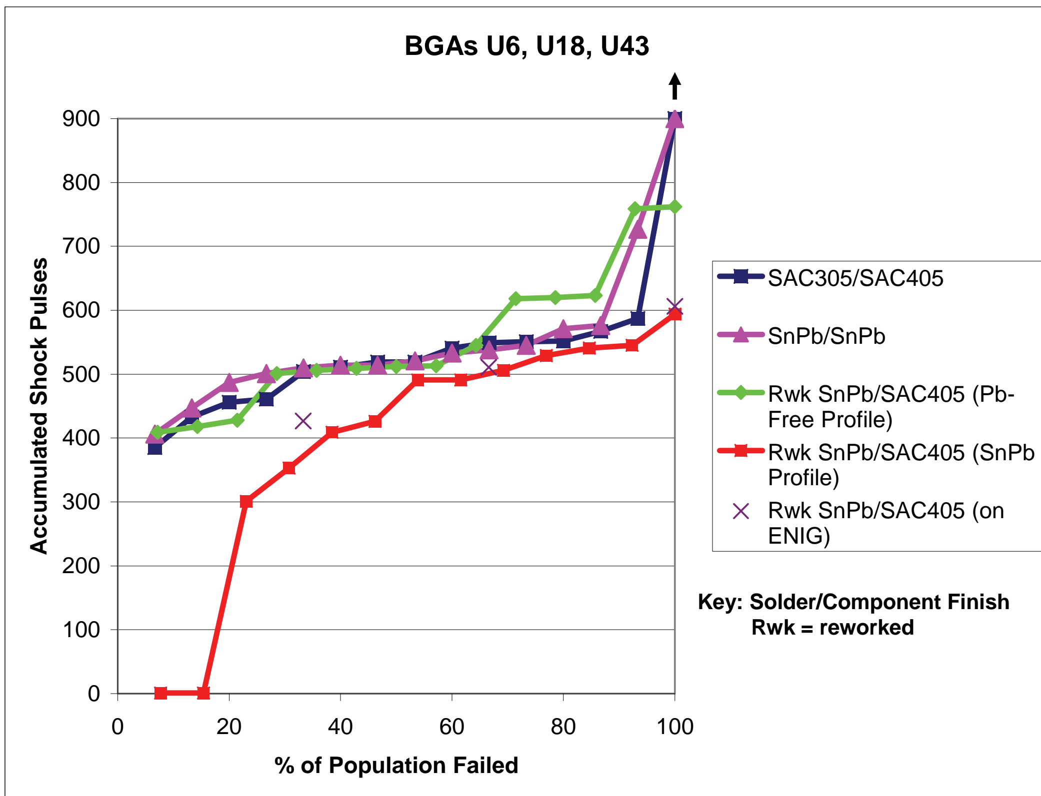

Figure 16. Combined Data from BGA's U6, U18, and U43

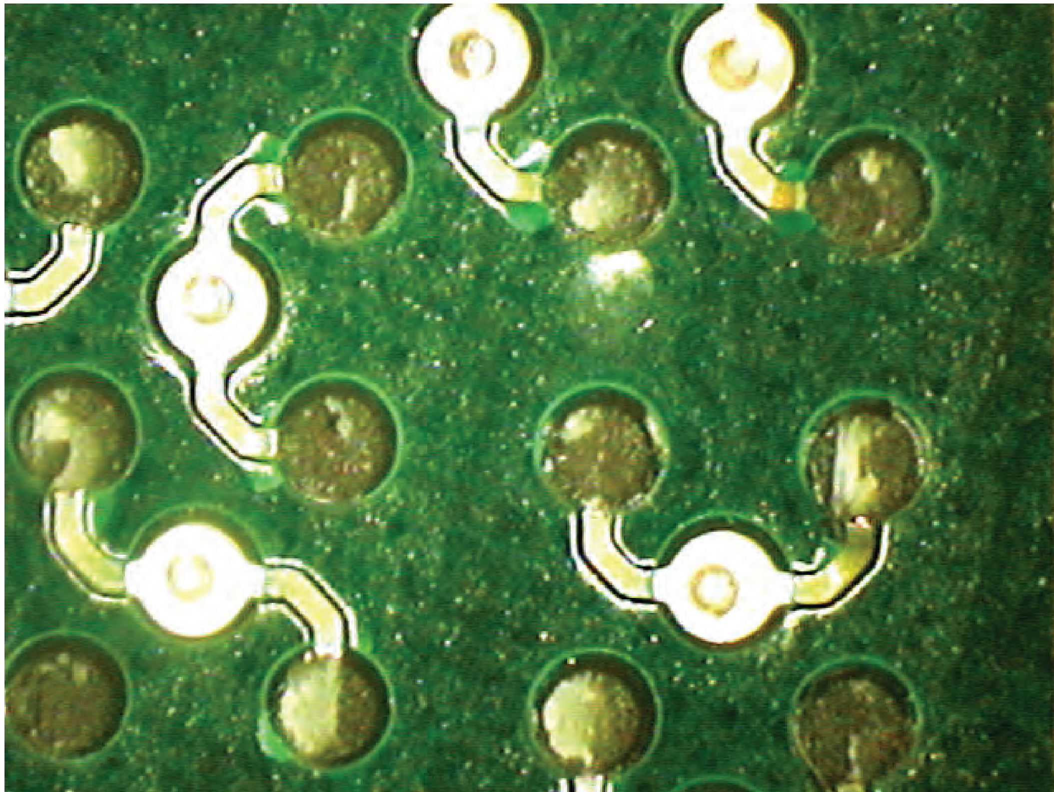

Figure 17. BGA U4 with Missing Pads (SnPb Solder/SnPb Balls)

No SAC305/SAC405 BGA's fell off during the test. The only purely lead-free BGA that fell off was one reworked using flux only and a BGA with SAC405 balls. For this BGA, 16% of the balls remained with the PWB with the solder joints failing on the component side (although most of the remaining balls also showed signs of PWB pad cratering). The balance of the BGA balls and associated PWB copper pads were missing from the test vehicle.

For the SAC305/SnPb, SnPb/SAC405, and reworked SnPb/SAC405 BGA's that fell off during testing, most of the BGA balls and associated PWB copper pads were missing from the test vehicles. The use of a SnPb versus a lead-free thermal profile for rework of the SnPb/SAC405 BGA's didn't appear to influence the failure mechanism.

The above failures were on test vehicles with an immersion Ag board finish. In contrast, the failure mechanism was different for the SnPb/SAC405 and reworked SnPb/SAC405 BGA's that fell off of the one ENIG board. Between 47 and 54% of the BGA balls remained on the test vehicle, which shows a shifting of the failures to the component side of the solder balls. Although the balance of the BGA balls were missing from the test vehicles, the majority of the copper pads were still attached to the PWB.

CLCC-20's

The SnPb/SnPb controls outperformed the combinations of SAC305/SAC305, SnPb/SAC305, and SAC305/SnPb (See Figure 18).

The amount of Pb detected in the SnPb/SAC305 and SAC305/SnPb solder joints was 24.7% and 16.5%, respectively (from ICP spectroscopy, see Table 3).

Figure 19 shows a typical crack in a CLCC solder joint.

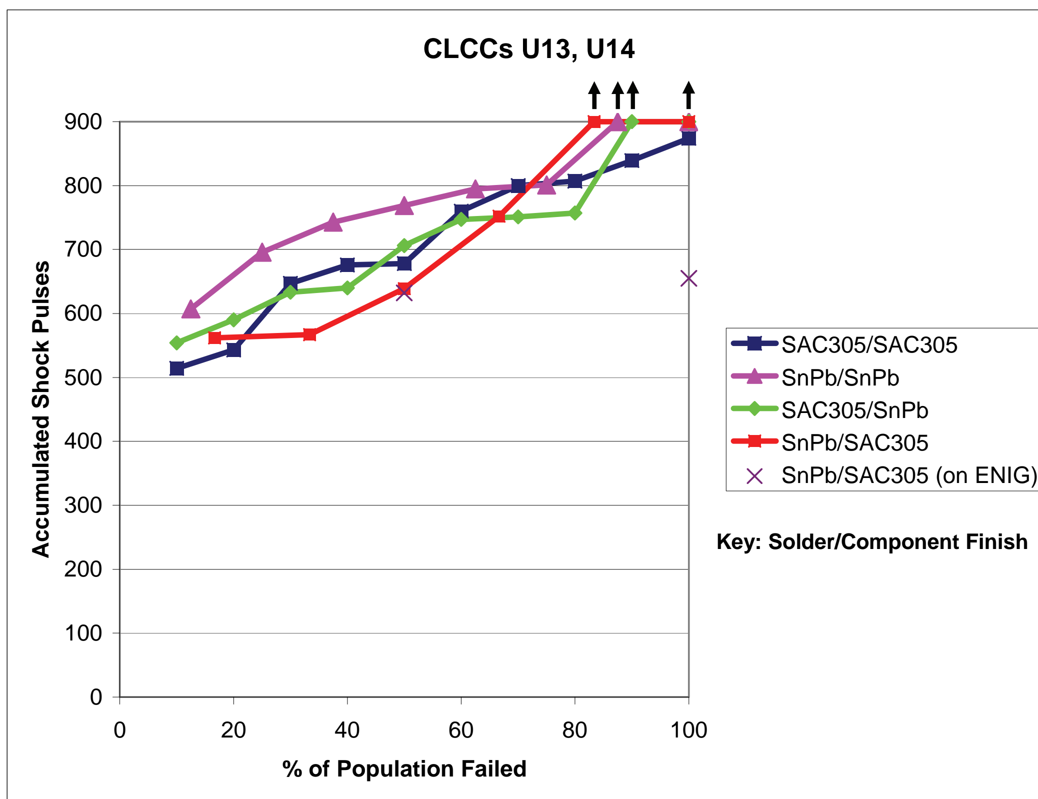

Figure 18. Combined Data from CLCC's U13 and U14

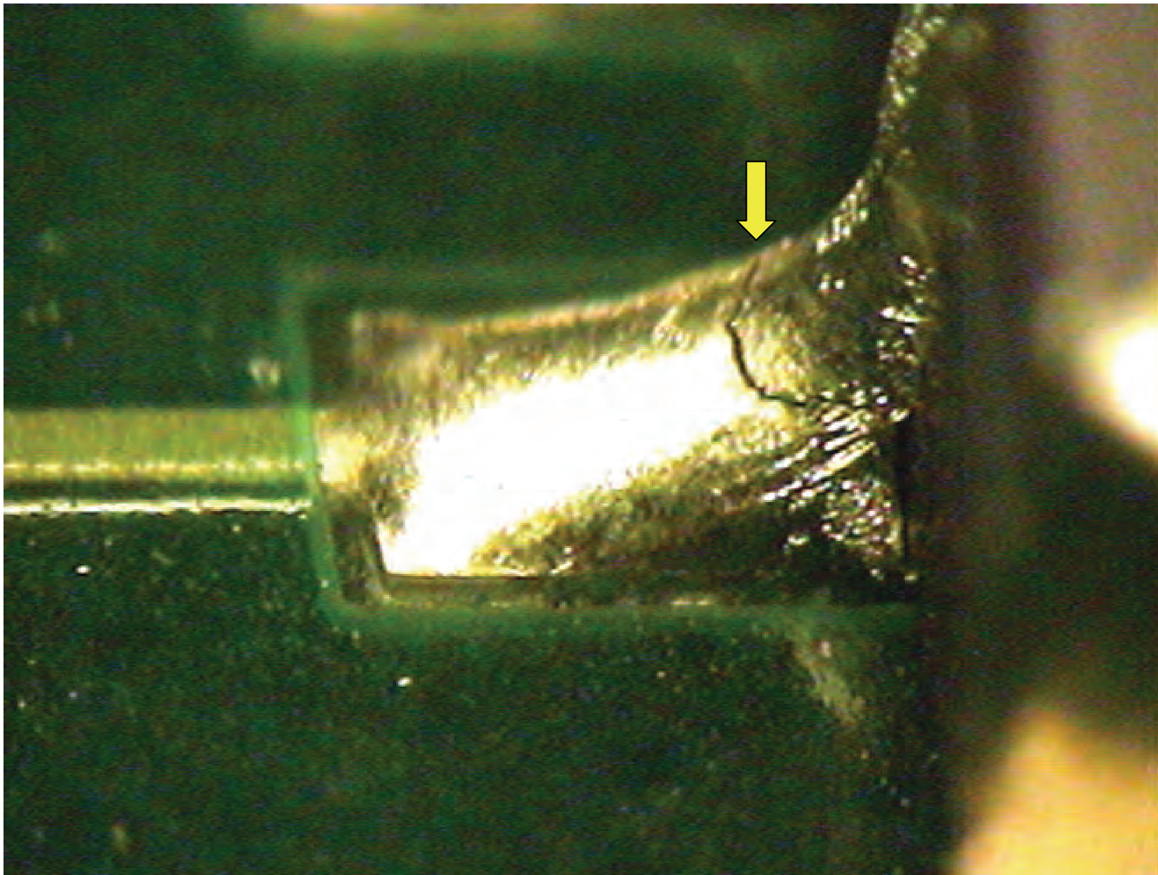

Figure 19. CLCC U10 with Cracked Solder Joint (SnPb/SAC305)

CSP-100's

The CSP daisy chain pattern on the test vehicles was incorrect with the result that only the outer perimeter balls of each CSP formed an electrically continuous path. In order for a CSP to be detected as failed, both legs of the outer perimeter needed to fail.

The relative ranking of the CSP solder/finish combinations was hindered because the CSP's at some locations had few or no failures. Therefore, the following rankings are somewhat subjective.

The combination of SAC305 solder/SAC105 balls generally performed as well as the SnPb/SnPb controls in mechanical shock. Micro sections made at the end of the test showed that the corner solder joints failed first. The SnPb/SnPb solder joints formed cracks primarily on the component side. The SAC305/SAC105 solder joints formed cracks primarily on the component side and also showed evidence of pad cratering (see Figure 20).

The combination of SAC305 solder/SnPb balls also performed almost as well as the SnPb/SnPb controls. In contrast, the combination of SnPb solder/SAC105 balls underperformed the SnPb/SnPb controls on either an immersion silver or ENIG board finish. These SnPb/SAC105 components were reflowed using a SnPb reflow profile.

The SnPb/SnPb CSP's reworked with flux only/SnPb balls were less reliable than the SnPb/SnPb control CSP's while the SAC305/SAC105 CSP's reworked with flux only/SAC 105 balls performed about as well the SnPb/SnPb control CSP's.

SnPb/SnPb CSP's reworked with SnPb/SAC105 and the SAC305/SAC105 CSP's reworked with SnPb/SAC105 underperformed the SnPb/SnPb controls. The former were reworked with a SnPb thermal profile while the latter were reworked with a Pb-free thermal profile which should have allowed complete mixing of the solders.

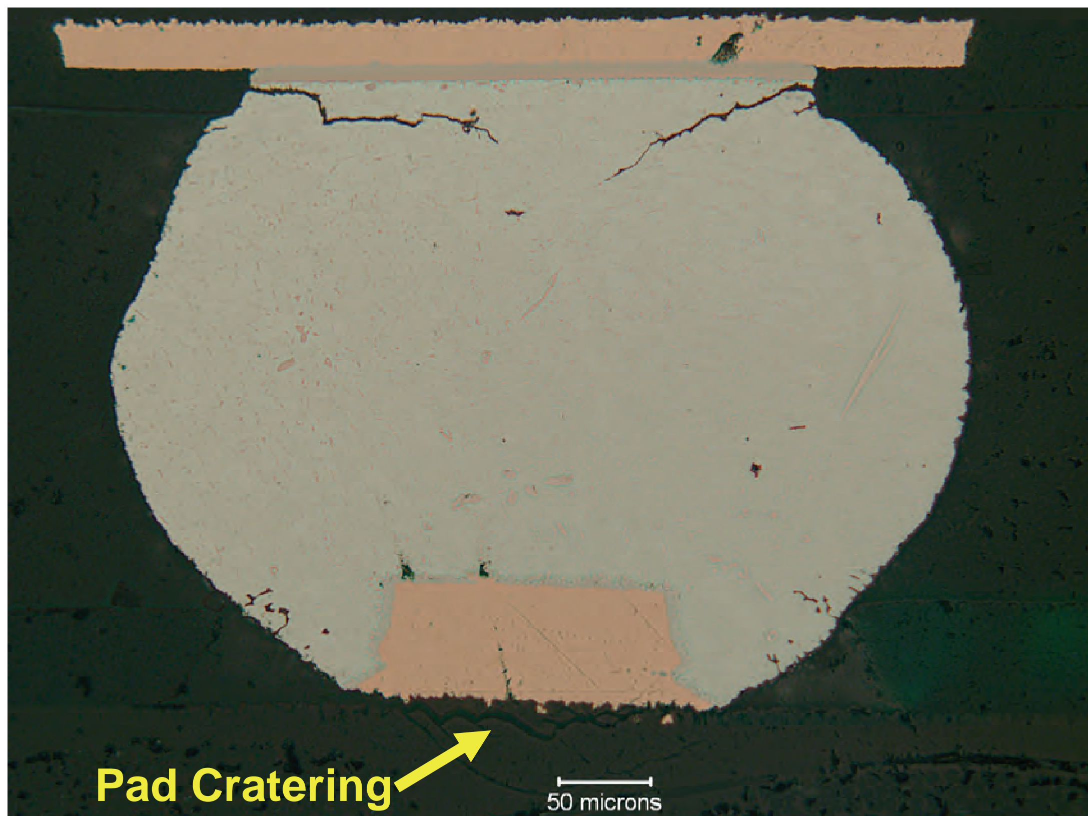

Figure 20. CSP U33 Corner Ball (SAC305 Solder/SAC105 Balls)

PDIP-20's
Two component finishes were used on the test vehicles (Sn and NiPdAu).

The combination of SN100C solder/Sn component finish generally performed as well as the SnPb/SnPb controls in mechanical shock (see Figure 21) although some of the the SN100C/Sn solder joints failed early. Microsections made at the end of the test showed that the corner solder joints failed first. The topside solder fillet would crack first followed by cracking of the lead where it necks down at the top of the PTH (see Figure 23). Another observation is that many of the PDIP's soldered with SN100C exhibited trace cracking at the corner solder joints (see Figure 24). This failure mode was not observed with the PDIP's assembled with SnPb solder.

The SnPb/SnPb PDIP's reworked with SnPb/Sn and the SN100C/Sn PDIP's reworked with SN100C/Sn were less reliable than the unreworked SnPb/SnPb control PDIP's (Figure 22).

Several of the earliest failures on the "Manufactured" test vehicles were SN100C/Sn solder joints. One possible cause is that some of the SN100C joints did not have a substantial topside solder filet. This could have resulted in a point of high stress concentration where the PDIP lead necked down resulting in premature failure of the lead. The trace cracking mentioned above is another possible cause for the early failures. The PDIP's that failed early exhibited both types of defects so it could not be definitively determined which occurred first.

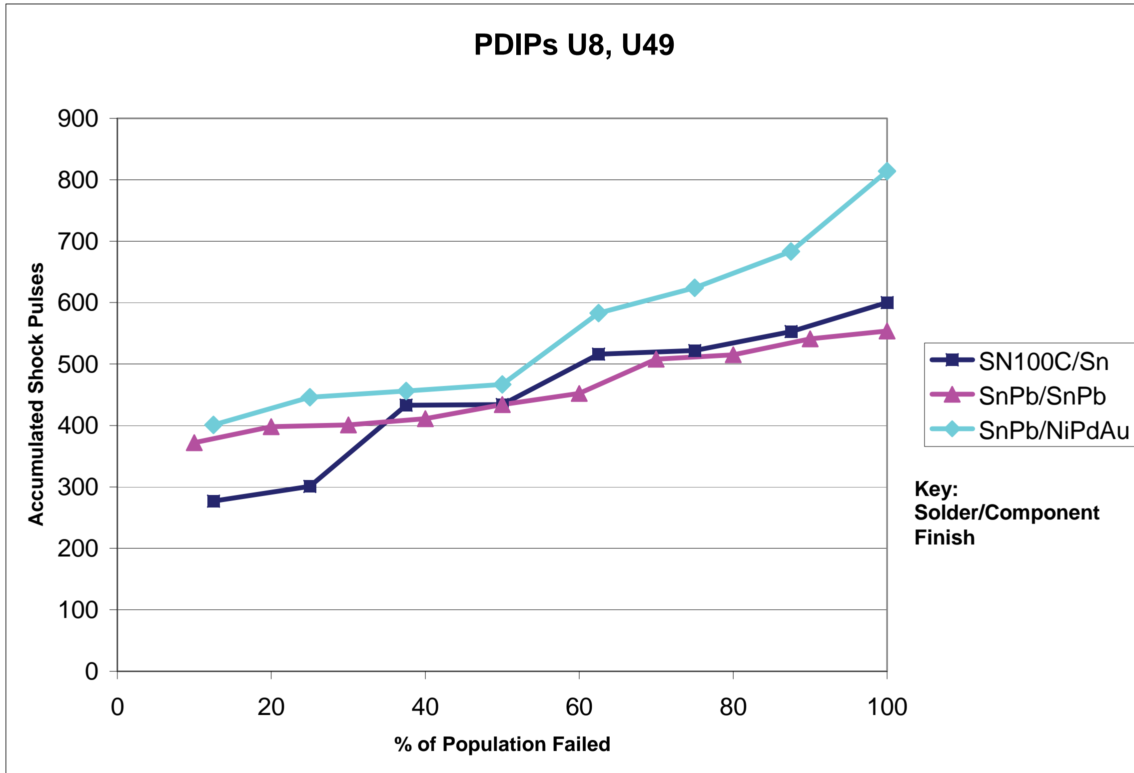

Figure 21. Combined Data from PDIP's U8 and U49

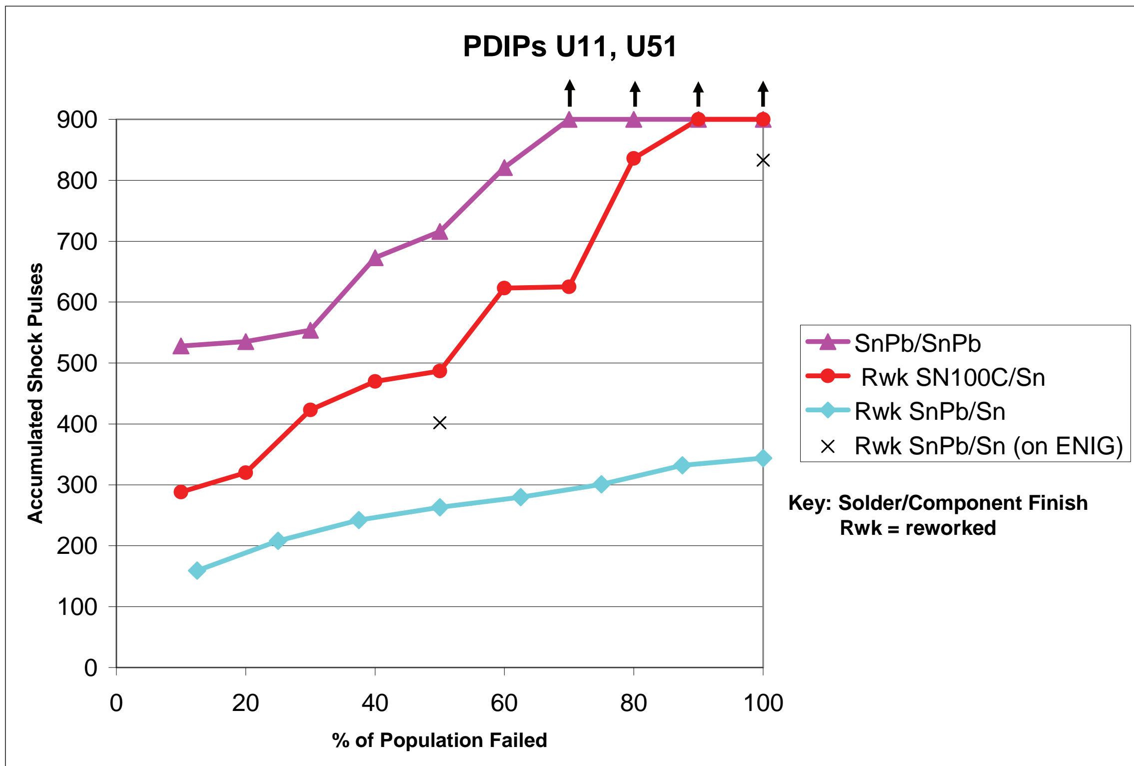

Figure 22. Combined Data from PDIP's U11 and U51

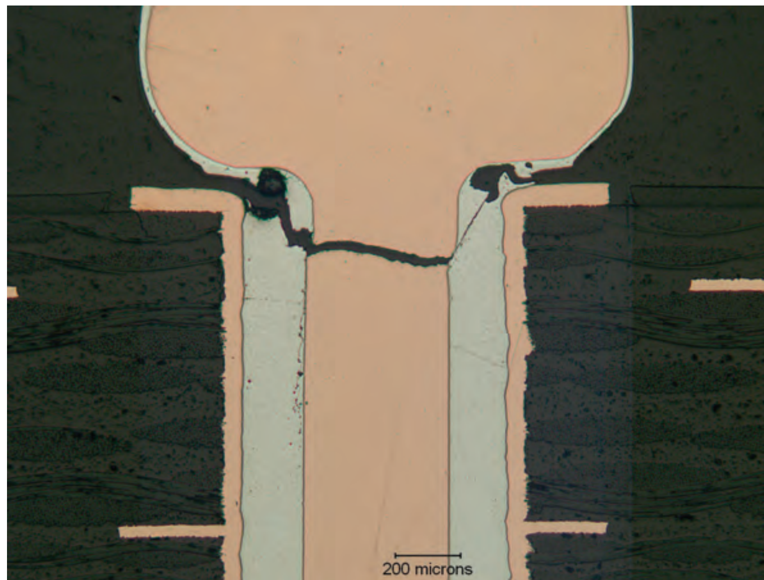

Figure 23. PDIP U8 Corner Lead (SN100C Solder/Sn Finish)

Figure 24. PDIP U38 (SN100C)

QFN-20's

The QFN's were resistant to failure under the conditions of this test. Only two QFN's failed (on Shocks 827 and 873) and they were both SAC305/Sn. Not enough failures occurred to rank the solders.

TQFP-144's

Most of the TQFP-144's had broken and/or missing leads at the end of the test (Figure 25). Since most of the failures appeared to be due to broken leads, the scatter in the test data for all of the TQFP solder/finish combinations was small. SAC305/Sn was equivalent in performance to SnPb/Sn, SnPb/NiPdAu (on immersion Ag), and SnPb/NiPdAu (on ENIG). SAC305/NiPdAu was slightly superior to the SnPb/Sn controls in performance (see Figure 26).

For this test, some Sn-plated TQFP-144 leads were dipped into either molten SnPb or SAC305 to evaluate the effectiveness of the hot solder dipping on tin whisker formation. The combination of SnPb/SnPb Dip was equivalent to the SnPb/Sn control in performance but the SAC305/SAC305 Dip performance was inferior to that of the SnPb/Sn control due to some early failures (Figure 27).

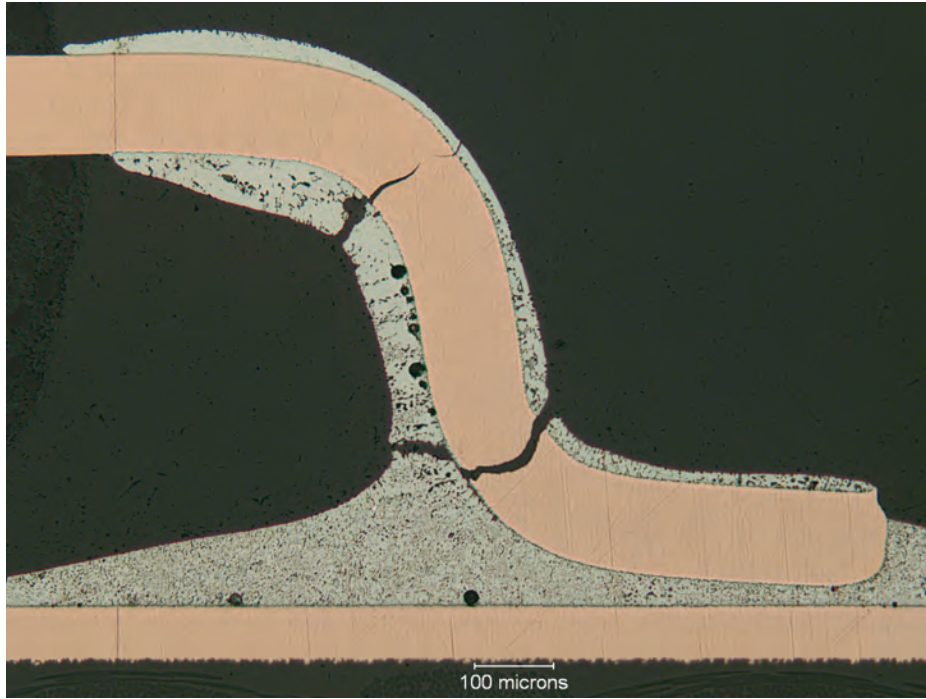

Figure 25. TQFP U7 Corner Lead (SnPb Solder/Sn Finish)

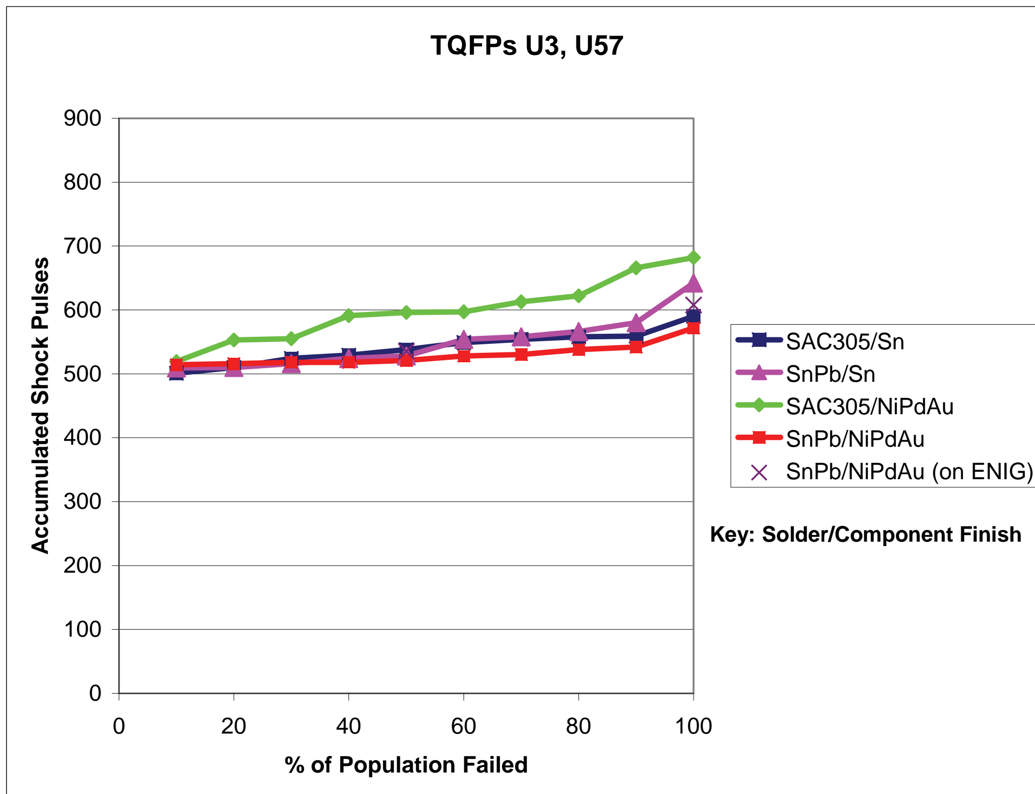

Figure 26. Combined Data from TQFP's U3 and U57

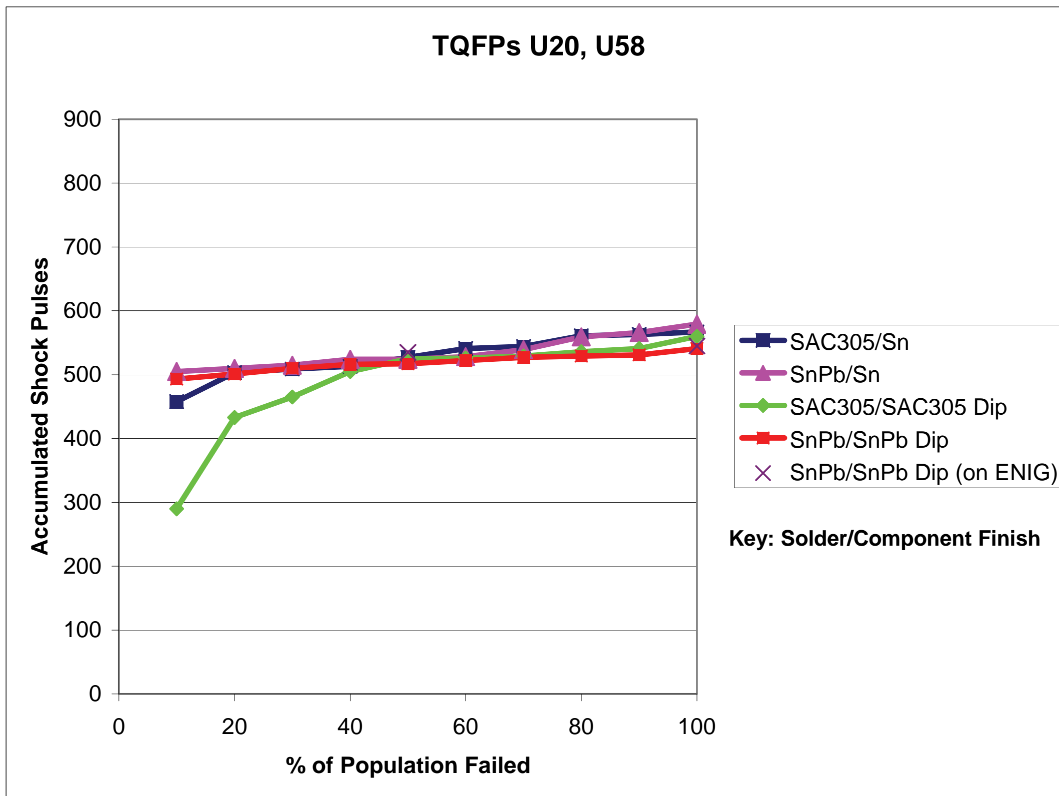

Figure 27. Combined Data from TQFP's U20 and U58

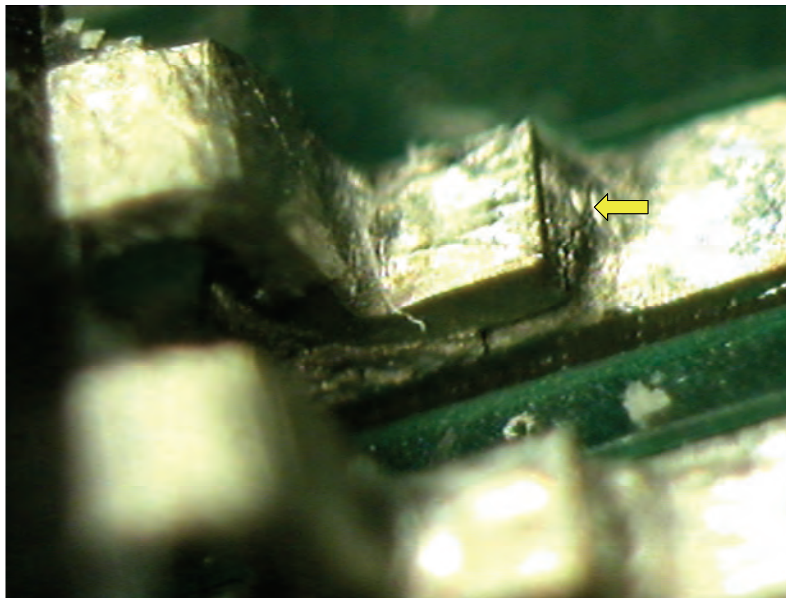

Figure 28. TSOP U61 Cracked Solder Joint (SnPb/SnPb)

TSOP-50's

The TSOP's that were not reworked were resistant to failure under the mechanical shock conditions of this test and the lack of failures made it impossible to rank the solder/finish combinations (i.e., SnPb/SnPb, SnPb/Sn, SAC305/Sn, and SAC305/SnBi). Unreworked SnPb/Sn on ENIG did have a few failures but they occurred late in the test.

Mixed solder/finish combinations also had few failures (i.e., SnPb/SnBi and SAC305/SnPb).

Rework had a definite negative effect on performance. SnPb/SnPb reworked with SnPb/SnPb and SAC305/Sn reworked with SnPb/Sn underperformed the unreworked SnPb/SnPb controls.

SnPb/SnPb reworked with SnPb/Sn and SAC305/SnBi reworked with SAC305/SnBi underperformed the unreworked SnPb/SnPb and SAC305/SnBi controls.

Figure 28 shows a typical crack in a TSOP solder joint.

Plated Through Holes (PTH's)
No PTH failures were observed.

Summary
The overall results of the mechanical shock testing are summarized in Table 6. If a solder alloy/component finish combination performed as well or better than the SnPb control, it was assigned the number "1" and the color "green". Solders that performed worse than the SnPb control were assigned a "2" and the color "yellow". For those cases where both the SnPb controls and a Pb-free solder had few or no failures after 900 shock pulses, they were not ranked.

Table 6. Ranking of Solder Alloy/Component Finish Combinations

	Relative Ranking (Solder/Finish)							
Component	Sn37Pb/Sn37Pb	SAC305/SAC405	Sn37Pb/SAC405	SAC305/Sn37Pb	Rwk Flux Only/Sn37Pb	Rwk Flux Only/SAC405	Rwk Sn37Pb/SAC405 (SnPb Profile)	Rwk Sn37Pb/SAC405 (Pb-Free Profile)
BGA-225	1	1	2	1	1	1	2	1

Component	Sn37Pb/Sn37Pb	SAC305/SAC305	Sn37Pb/SAC305	SAC305/Sn37Pb
CLCC-20	1	2	2	2

Component	Sn37Pb/Sn37Pb	SAC305/SAC105	Sn37Pb/SAC105	SAC305/Sn37Pb	Rwk Flux Only/Sn37Pb	Rwk Flux Only/SAC105	Rwk Sn37Pb/SAC105 (SnPb Profile)	Rwk Sn37Pb/SAC105 (Pb-Free Profile)
CSP-100	1	1	2	1	2	1	2	2

Component	Sn37Pb/SnPb	SN100C/Sn	Sn37Pb/NiPdAu	Rwk Sn37Pb/Sn	Rwk SN100C/Sn
PDIP-20	1	1	1	2	2

Component	Sn37Pb/Sn37Pb	SAC305/Sn	Sn37Pb/Sn	SAC305/Sn37Pb
QFN-20	Not enough failures to rank	Not enough failures to rank	Not enough failures to rank	Not enough failures to rank

Component	Sn37Pb/Sn	SAC305/Sn	Sn37Pb/NiPdAu	SAC305/NiPdAu	Sn37Pb/Sn37Pb Dip	SAC305/SAC305 Dip
TQFP-144	1	1	1	1	1	2

Component	Sn37Pb/SnPb	Sn37Pb/Sn	Sn37Pb/SnBi	SAC305/Sn	SAC305/SnBi	SAC305/SnPb	Rwk Sn37Pb/SnPb	Rwk Sn37Pb/Sn (SnPb Profile)	Rwk Sn37Pb/Sn (Pb-Free Profile)	Rwk SAC305/SnBi
TSOP-50	Not enough failures to rank	Not enough failures to rank	Not enough failures to rank	Not enough failures to rank	Not enough failures to rank	Not enough failures to rank	2	2	2	2

Key: Solder/Component Finish
Rwk = reworked

The rankings in Table 6 are somewhat subjective since the data for some component types contained a lot of scatter and other component types had few failures which complicated the ranking process. In addition, if some of the component/solder combinations had only a few early failures, these failures did not count in the ranking process.

In general, the pure lead-free systems (SAC305/SAC405 balls, SAC305/SAC105 balls, SAC305/Sn, and SN100C/Sn) perfomed as well or better than the SbPb controls (SnPb/SnPb or SnPb/Sn).

For mixed technologies, SnPb solder balls combined with SAC305 paste (and reflowed with a Pb-free profile) perfomed as well as the SnPb controls on both the BGA's and the CSP's. In contrast, SnPb solder paste combined with either SAC405 or SAC105 balls (and reflowed with a SnPb thermal profile) underperformed the SnPb/SnPb controls.

Rework operations on the PDIP's and TSOP's reduced the reliability of both the SnPb and the Pb-free solders when compared to the unreworked SnPb/SnPb controls. In contrast, rework of SnPb and SAC405 BGA's and SAC105 CSP's using flux only gave equivalent performance to the unreworked SnPb/SnPb controls. Pb-free BGA's reworked with SnPb paste and SAC405 balls (and a Pb-free thermal profile) were also equivalent to the SnPb controls.

Many of the BGA failures (SnPb/SbPb balls, SAC305/SAC405 balls, and mixed technologies) were due to pad cratering. This suggests that lead-free laminates may be the weakest link for large area array components.

Conclusions and Recommendations

The results of this study suggest that for most component types, the lead-free solders tested are as reliable as eutectic SnPb solder with respect to mechanical shock. Most of the components tested (including reworked components) successfully passed the tests defined in MIL-STD-810G 33 times each no matter which solder was used. These tests are the Functional Test (Flight Equipment); the Functional Test (Ground Equipment); and the Crash Hazard Test (Ground Equipment).

These results suggest that the Pb-free solders tested can be used on designs that will be exposed to mechanical shock and will perform as well as currently used eutectic SnPb solder under many use conditions.

Acknowledgements

Thanks to Tom Kowalski for running the electrodynamic shaker and collecting accelerometer and strain gage data. Thanks to Don Powers for designing the fixture, conducting the laser vibrometer modal analysis, and collecting laser data for the full field strain calculations. Thanks to John Packard for his microsections. A special thanks to Nihon Superior for funding testing of the "Manufactured" test vehicles and to the Boeing PSS Domain for funding the testing of the "Rework" test vehicles.

References

1. NASA-DoD Lead-Free Electronics Project Plan, August 2009.
2. Woodrow, Tom; "NASA-DoD Lead-Free Electronics Project: Mechanical Shock Test", Boeing Electronics Materials and Processes Report – 602, January 4, 2010 (this report can be found at http://www.acqp2.nasa.gov/NASA_DOD LeadFreeElectronics_Proj2.html).
3. MIL-STD-810G, "Environmental Engineering Considerations and Laboratory Tests", 31 October 2008.